NGR 43-002-031

ANALYSIS OF THE FLOW FIELD GENERATED NEAR AN AIRCRAFT ENGINE OPERATING IN REVERSE THRUST

DRA

VANDERBILT UNIVERSITY

WALTER ANDREW LEDWITH, JR.

August, 1972

DEPARTMENT OF MECHANICAL ENGINEERING
SCHOOL OF ENGINEERING

(NASA-CR-121147) ANALYSIS OF THE FLOW FIELD GENERATED NEAR AN AIRCRAFT ENGINE OPERATING IN REVERSE THRUST M.S. Thesis (Vanderbilt Univ.) 95 p HC $6.75 CSCL 20D G3/12

N73-18264

Unclas
16525

ANALYSIS OF THE FLOW FIELD GENERATED NEAR AN AIRCRAFT ENGINE OPERATING IN REVERSE THRUST

By

Walter Andrew Ledwith, Jr.

Thesis

Submitted to the Faculty of the

Graduate School of Vanderbilt University

in partial fulfillment of the requirements

for the degree of

MASTER OF SCIENCE

in

Mechanical Engineering

August, 1972

Nashville, Tennessee

Approved: Date:

SUMMARY

This thesis develops a computer solution to the exhaust gas reingestion problem for aircraft operating in the reverse thrust mode on a crosswind-free runway. The computer program determines the location of the inlet flow pattern, whether the exhaust efflux lies within the inlet flow pattern or not, and if so, the approximate time before the reversed flow reaches the engine inlet. The program is written so that the user is free to select discrete runway speeds or to study the entire aircraft deceleration process for both the farfield and cross-ingestion problems. While developed with STOL applications in mind, the solution is equally applicable to conventional designs.

The inlet and reversed jet flow fields involved in the problem are assumed to be non-interacting. The nacelle model used in determining the inlet flow field is generated using an iterative solution to the Neuman Problem from potential flow theory while the reversed jet flow field is adapted using an empirical correlation from the literature. Sample results obtained using the program are included.

ACKNOWLEDGEMENTS

I would like to thank my advisor, Dr. John W. Tatom, for suggesting this topic and for the assistance he gave me during the course of this investigation. I would also like to thank Dr. Norman M. Schnurr and Dr. Hugh F. Keedy for their help and for reading the manuscript.

This work was partially supported by NASA Grant NGR 43-002-034.

TABLE OF CONTENTS

Page

LIST OF ILLUSTRATIONS

LIST OF TABLES

NOMENCLATURE

Symbol	Definition
A' [1]	Area, ft^2
AL'	Nacelle length, ft
CHEKX	Normal velocity on the end cap
CHEKR	Normal velocity on the nacelle
D'	Distance between two points, ft
D1'	Distance between a point of interest in space and a point on the engine inlet, ft
D2'	Distance between a point of interest in space and a point on the nacelle, ft
D3'	Distance between a point of interest in space and a point on the end cap, ft
DIAJET	Diameter of the reversed jet at the point of origin
DSAB	Distance between points "a" and "b"
EP	Nacelle generation no-flow criteria - a select percentage of the freestream velocity
g'	Number of singularities per unit area, ft^{-2}
$\dot{m}'$	Strength of a singularity, ft^3/sec
PMPP	The "P" coordinate in the jet plane of the Maximum Penetration Point of the reversed jet

---

[1] In this work, primes indicate dimensional quantities while non-primes indicate dimensionless quantities. Velocity and length terms are non-dimensionalized by referring them, respectively, to the freestream velocity U_∞' and to the nacelle radius R'. The product of $U_\infty'R'$ is used to non-dimensionalize the velocity potential and stream function terms.

Symbol	Definition
Q'	Volumetric flow rate from a singularity, ft^3/sec
QMPP	The "Q" coordinate in the jet plane of the Maximum Penetration Point of the reversed jet.
qsl'	The strength of the inlet sink, ft^3/sec
r	A radial space coordinate
r3	A radial space coordinate on the model nacelle
RA	Radius of point "a"
RAB	Radial distance between points "a" and "b"
RB	Radius of point "b"
RCROSS	Radius of the Maximum Penetration Point of the reversed jet of an adjacent engine on the coordinate system of an engine under study
RMPP	Radial coordinate of the Maximum Penetration Point of the reversed jet
RPEST	Radius of the pre-entry streamtube at an infinite axial location upstream of the engine inlet
s_J	A velocity component of VELJET
TAB	The time required for a tracer particle to go between points "a" and "b", $(TAB')(U_\infty')/(R')$
u_J	A velocity component associated with VELJET
V	Velocity
VAB	The average velocity of a tracer particle between points "a" and "b"
VAX	A normal velocity produced by a singularity on the end cap
VAXY	The axial velocity at any point in space

Symbol	Definition
VELJET	The velocity of the reversed jet
VELRAT	The inlet-to-freestream velocity ratio, $qs1'/(2 \cdot U_\infty')$
V_n'	A normal surface velocity, ft/sec
VP	Velocity at a point
VPA	Velocity at point "a"
VPB	Velocity at point "b"
Vr	The normal velocity produced by a singularity on the nacelle
VRAD	The radial velocity of any point in space
w_J	A velocity component of VELJET
x	An axial space coordinate
x1	An axial space coordinate along the nacelle
XA	The axial coordinate of point "a"
XAB	The axial distance between points "a" and "b"
XB	The axial coordinate of point "b"
XJET	The axial coordinate of the reversed jet origin
XMPP	The axial coordinate of the Maximum Penetration Point of the reversed jet
XOP	The axial coordinate of the Maximum Penetration Point of the reversed jet of an adjacent engine on the coordinate system of an engine under study
XSPACE	The "x" component of the distance between the end cap center points of two adjacent engines
y	A space coordinate

Symbol	Definition
y1	A space coordinate on the nacelle
YJET	A coordinate of the reversed jet exhaust origin
YMPP	A coordinate of the Maximum Penetration Point of the reversed jet
YOP	A coordinate of the Maximum Penetration Point of the reversed jet of an adjacent engine on the coordinate system of an engine under study.
YSPACE	The "y" component of the distance between the end cap center points of two adjacent engines
z	A space coordinate
z1	A space coordinate on the nacelle
ZJET	A coordinate of the reversed jet exhaust origin
ZMPP	A coordinate of the Maximum Penetration Point of the reversed jet
ZOP	A coordinate of the Maximum Penetration Point of the reversed jet of an adjacent engine on the coordinate system of an engine under study
ZSPACE	The "z" component of the distance between the end cap center points of two adjacent engines
$\alpha 1$	The exhaust jet pitch angle
$\alpha 2$	The exhaust jet turning angle
β	Angle between the reversed jet and the x-y plane
θ	The angle in the jet plane that the reversed jet makes with the "P" axis
$\theta 1$	Angular space coordinate
φ	Velocity potential

Symbol	Definition
φ_1	Velocity potential associated with the freestream-inlet combination
φ_{CAX}	Velocity potential associated with the distributed compensatory singularities on the end cap
φ_{CR}	Velocity potential associated with the distributed compensatory singularities on the nacelle
φ_{FS}	Velocity potential induced by the freestream
φ_S	Velocity potential induced by the inlet sink
Ψ	Stream function

CHAPTER I

INTRODUCTION

The forthcoming development of both military and commercial short take-off and landing (STOL) aircraft will have a significant impact on air transportation. Quiet, civil STOL aircraft will greatly diminish city-to-city travel times and help relieve present airport congestion by operating from short, inner city airstrips. Such airstrips will be inexpensive enough that jet transportation can be extended to small communities and underdeveloped countries alike. In military versions, STOL transports will greatly improve the ability to supply remote regions.

But before such a family of aircraft can be put into service there remain a number of problems to be resolved. One of the more important areas is the need for better thrust reversers. Unlike conventional aircraft, the normal means of stopping both military and commercial STOL's will most likely be through the use of reversers alone. For the military, the capability to brake with reversers alone will greatly enhance operation from unprepared airstrips, by avoiding the rutting problem associated with wheel braking. For the commercial user, efficient reverse thrust braking is a matter of both economics and safety. The high operating costs of such aircraft will demand maximum daily utilization for profitable operation. Not only is brake maintainance a major operating expense, but brake cooling requirements play a significant role in determining the aircraft turn-around time. From safety considerations, the full reverser stopping capability will improve operation from short, icy runways.

Though thrust reversers have been used on jet aircraft for years, none have achieved the full stopping capability. There are several reasons for this. First, unlike STOL aircraft, conventional aircraft do not have sufficient thrust-to-weight ratios to stop within reasonable distances without the simultaneous use of wheel brakes. Secondly, the tendency of the engines to reingest their own reversed exhaust at low speeds has demanded that reverse thrust operation be terminated long before the aircraft has reached a halt. In addition to damaging parts, reingestion can cause compressor surge and greatly diminish the magnitude of the braking force. Thus any practical STOL aircraft must be designed to operate in reverse thrust, free of exhaust gas reingestion down to very low ground speeds.

The purpose of this thesis is to develop an analytical model of the flow field near an aircraft engine operating in reverse thrust on a crosswind-free runway and to predict whether exhaust gas reingestion will occur. The study provides a tool, in the form of a computer program, to be used in the design of engine-nacelle-reverser systems. The designer is free to choose whatever dynamic and geometric conditions he wishes and can then see how effective they are with regard to the reingestion problem.

The overall flow field in this problem can be divided into two regimes:

1. the inlet flow field which is basically potential, and
2. the reversed jet flow field which is highly turbulent.

Ordinarily, the presence of two such diverse flow fields would make the development of any single analytical model an enormously difficult task. But in this investigation the two are mathematically uncoupled and solved separately. This greatly simplifies the analysis.

There are several basic types of exhaust gas reingestion. The first type is near-field reingestion which occurs when the exhaust efflux passes too close to the nacelle. Because of the Coanda effect, the reversed jet attaches to the nacelle and subsequently enters the engine inlet. A second type is farfield reingestion where the jet penetrates the engine inlet flow pattern. A third type is cross-ingestion, where the reversed jet penetrates the inlet flow pattern of an adjacent engine.

The computer program presented here is designed to study the latter two cases. It will not analyze the first case since no relavent studies of nacelle attachment currently exist. Therefore all solutions generated by this program are based on the assumption that the near-field problem does not occur.

The basic case under study is that of a turbofan engine installed in a long-duct nacelle, with a target reverser simultaneously handling the fan and core engine flows. One reason for selection of this configuration is its superiority in reducing approach and sideline engine noise. This currently is an important consideration since to receive community acceptance STOL aircraft will have to be significantly quieter than conventional aircraft.

CHAPTER II

PAST RESEARCH EFFORTS

A search of the literature failed to reveal a past analytical solution to the thrust reverser reingestion problem. The solution presented here is based on a method proposed by Tatom [1].[1] This method employs an axisymmetric model of an engine nacelle discharging round, turbulent, reversed jets[2] and is described in detail in the next chapter.

Because of the importance of mathematically uncoupling the inlet and reversed-jet flow fields in Tatom's method, an investigation of the validity of this simplification was first made. It appears that the concept is well founded since there is ample evidence that:

1. The effect of the presence of the reversed jet on the freestream is small (i.e., the freestream flow near the jet is essentially the same with and without the jet).

---

[1] Numbers in brackets indicate references cited in the Bibliography.

[2] Jet effluxes from target type reversers tend to be approximately round in cross-section.

2. The effect of the engine inlet suction on the reversed jet is small (i.e., the trajectory of the jet is essentially the same with and without the presence of the inlet).

Keffer and Baines [2] studied round turbulent jets introduced normally into a freestream. It was observed that the freestream was unaffected by the presence of the jet and that in the vicinity of the jet the static pressure and mean velocity of the freestream could be considered constant. Additional evidence of non-interaction between the jet and the freestream can be found in the report by Weiss and McGuigan [3]. This paper contains oil-streak photographs of cold-flow tests of a model reverser-nacelle configuration. In each of these photographs the freestream is essentially parallel at a distance of less than 2 jet diameters upstream of the deflected jet.

In each of the references cited above, the jets were discrete and thus produced relatively small blockage of the freestream flow field. The works of Cooper [4] and Hayden [5] are concerned with a two-dimensional reverser model with a simulated engine inlet. In this study the reversed jet blocked the entire freestream flow. Nowhere was the inlet flow field far removed from the reverser flow field. Yet flow visualization photographs of the reversed jet and temperature and velocity data taken with and without inlet suction, show no significant differences. These results further indicate that the freestream is almost unaffected by the presence of the jet. Thus the independence of the two flow fields is verified. Since a round jet occupies much less volume in the region of the inlet than a two-dimensional jet, it follows that the effect of the inlet on a round jet will also be small.

With the uncoupling hypothesis justified, attention is turned to previous efforts in the separate areas of inlet flow prediction and the trajectories of turbulent transverse jets.

The inlet flow portion of the reingestion problem can be described adequately from potential flow theory. The basic problem (the Neuman Problem) involves generating a mathematical model of the flow near an engine nacelle within a freestream. This could be done by employing the Douglas-Neuman Potential Flow Computer Program developed by A.M.O. Smith and J. Pierce [6]. This selection was not used in [1] for several reasons. First, the program was unavailable at the Vanderbilt University Computer Center and it was felt that adaptation of the program both to the Center's machine and to the reingestion problem would present as many difficulties as developing a new one. Secondly, it was felt that a new program might offer simplifications over the Douglas program and thus cost less to operate.

The remaining area to be discussed is concerned with studies of jets penetrating into a freestream. Unfortunately, most of the available literature is of little valve for two reasons:

1. The studies are concerned with deflection of and velocities along the jet centerline which are of little importance here. The principle area of concern in the reingestion problem is the maximum penetration of the jet into the free-stream.
2. The sutdies are concerned with jet-to-freestream angles and velocity ratios considerably different than those encountered in reverser applications. Several analytical studies of opposing jets exist [7, 8, 9], but these assume an incompressible, irrotational flow field.

The engine-nacelle model proposed in [1] incorporates the results of a Lockheed-Georgia study [10] to describe the reversed jets. The study was concerned with a round, turbulent jet introduced obliquely into an opposing freestream. Conducted in a low turbulence wind tunnel the experiment allowed the Maximum Penetration Point of the jet into the freestream to be photographically measured. The tests employed a wide range of values for the jet exit diameter, the jet-to-freestream velocity ratio, and the jet-to-freestream included angle. The result of this study was the Lockheed jet penetration correlation as presented in Figure 1, empirically relating the time averaged maximum

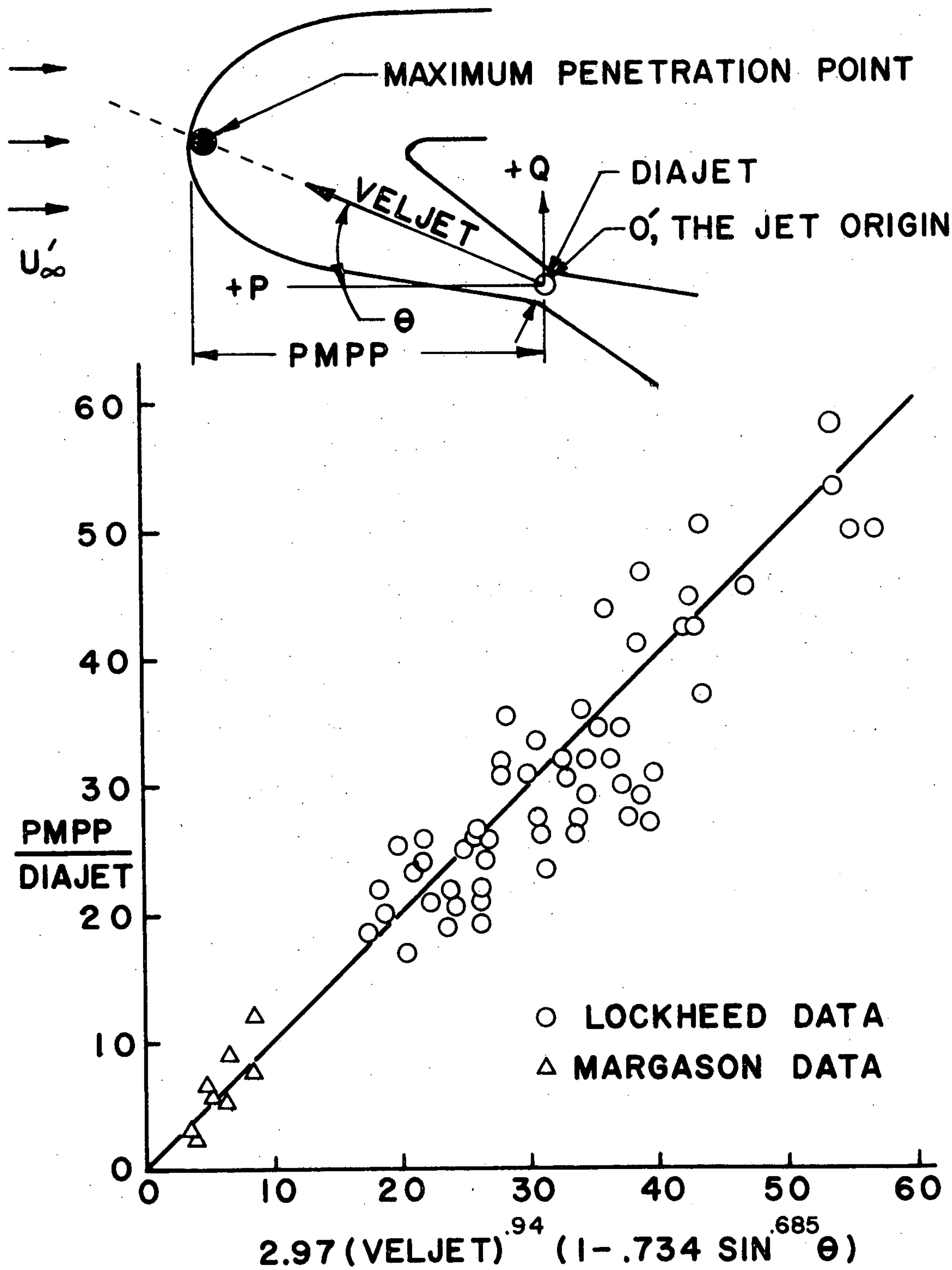

FIGURE 1. JET PENETRATION CORRELATION

penetration to the above menetioned variables. Additional data by Margeson [11] is also presented.

Figure 1 also shows a sketch of the reversed jet. Several characteristics of this jet should be noted. First, photographs indicate that the Maximum Penetration Point can be considered to lie approximately on an extension of the jet centerline. Secondly, the jet should not be considered as a fixed region in space. All flow visualization studies report that the reversed jet is an area of violent turbulence. Thus, the time-averaged Lockheed data does not show where the Maximum Penetration Point lies at any instant, but where it is most often found.

CHAPTER III

THEORY

An overall view of the flow field involved in the problem is shown in Figure 2. As has already been noted, this flow field can be divided into inlet and reversed-jet flow fields; these being respectively, potential and turbulent in nature. The uncoupling hypothesis allows the two to be treated as independent problems. Hence the inlet flow model appears as a fictitious engine ingesting air but producing no exhaust, while the exhaust flow model appears as an isolated turbulent jet discharging obliquely into an opposing freestream.

The inlet flow field is represented in the figure by the presence of the streamlines. Among these, the pre-entry streamtube is of special importance. This is defined such that fluid lying inside of it enters the engine while fluid lying outside of it travels past the nacelle.

The exhaust flow too, has an item of special importance: the Maximum Penetration Point. At this point, the axial momentum of the jet has been completely depleted so that additional axial travel is determined by the opposing freestream. If the Maximum Penetration Point lies within the pre-entry streamtube, exhaust gas will be carried into the engine inlet. This is the cause of farfield reingestion. The primary task of this investigation is to develop an analytical model capable of generating

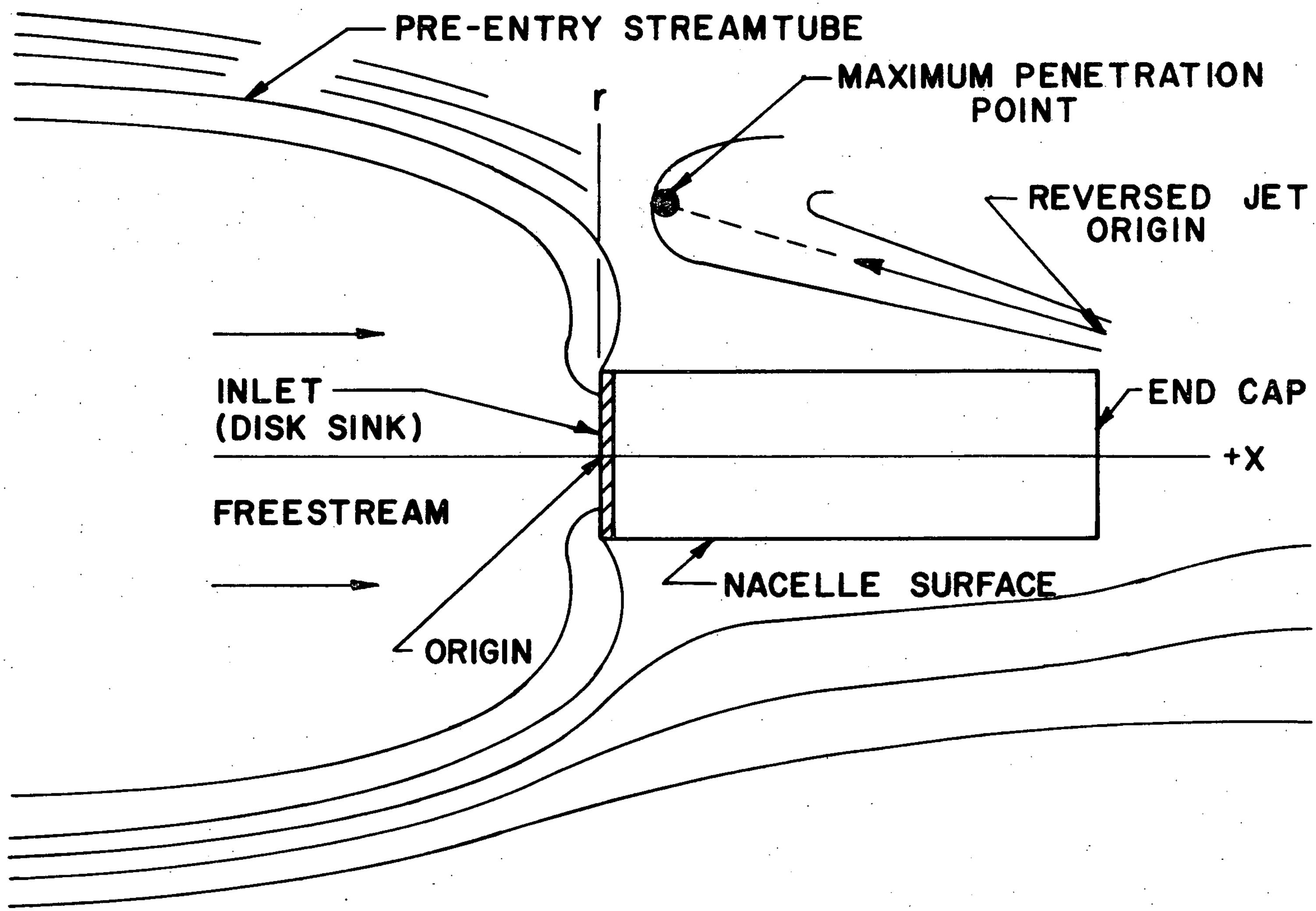

FIGURE 2. THE PHYSICAL SITUATION

the pre-entry streamtube and the Maximum Penetration Point, and determining whether or not the latter lies inside or outside of the former.[1]

The Inlet Flow Field Model

The inlet flow field solution is developed around a cylindrical nacelle configuration, with an end cap at the rear and a full frontal area inlet (Figure 2). This geometry differs somewhat from actual engines. First, the inlet cannot fill the entire frontal area in a real nacelle due to structural and aerodynamic considerations. Secondly, nacelles are not cylindrical but are more streamlined bodies of revolution. The approximate nacelle representation is used because of the mathematical simplifications and resulting savings in computer time it affords. These simplifications are not believed to decrease significantly the accuracy of the solution since, in the farfield problem, the area where reingestion begins is somewhat removed from the engine. However, it must be recognized that near the inlet, the nacelle contour materially influences the shape of the streamlines.

---

[1] It should be noted that up to the Maximum Penetration Point the jet is entraining, not releasing, fluid. Hence, it is premissible for the reversed jet to lie within the pre-entry streamtube, as long as the Maximum Penetration Point does not.

Any exact mathematical model should acknowledge the rapid deceleration involved in the reversing process. While a transient description of the flow fields is desirable, a method for developing one is unclear. Therefore, as a final simplification, it is assumed that the aircraft passes continuously through a series of equilibrium flow fields in coming to rest.

The purpose of the inlet flow field model is to generate the streamlines about the engine nacelle. The development of this model begins by placing a potential flow freestream (alligned with the axis) on an axisymmetric coordinate system to simulate the runway speed of the aircraft. The engine nacelle is generated within this freestream. Towards this end, an origin is established on the coordinate system and at this origin a disk sink is added to simulate the engine inlet (Figure 2).

In establishing the nacelle and end cap surfaces, a special set of boundary conditions must be satisfied. Because a real nacelle surface is solid, no fluid passes through it and hence the normal surface velocities must vanish. The same boundary condition applies along the end cap too, because the uncoupling assumption has removed the exhaust flow from the inlet model. The boundary conditions are satisfied by establishing a distributed system of compensatory singularities over the nacelle and end cap surfaces.

An iterative procedure is used to determine the singularity strengths. Initially, each singularity strength is set opposite and proportional to the normal velocity induced by the freestream-inlet combination at the point. This would be sufficient for compensation at isolated points. However, the presence of neighboring singularities induces an additional normal velocity at each point. These velocity components must also be cancelled and this is done by the iterative adjustment scheme.[2] Once the boundary conditions are satisfied the inlet flow field model is capable of generating streamlines.

The Reversed Jet Model

The purpose of the reversed jet model is to locate the Maximum Penetration Point of the exhaust flow. The geometry of the problem is shown in Figure 3, with the nacelle outline included for clarity. The centerline of the jet is considered to lie in a plane. This jet plane (the P-Q coordinate system in the figure) is defined by the freestream and reversed jet velocity vectors and has its origin (o') at the point of reversed exhaust discharge. It is in this plane that the Lockheed correlation applies.

---

[2] The surface generation process discussed here and proposed in [1] evolved from the analysis of [12]. The major computational difference between the two is that the latter makes no attempt at eliminating the normal velocity component induced by the neighboring singularities.

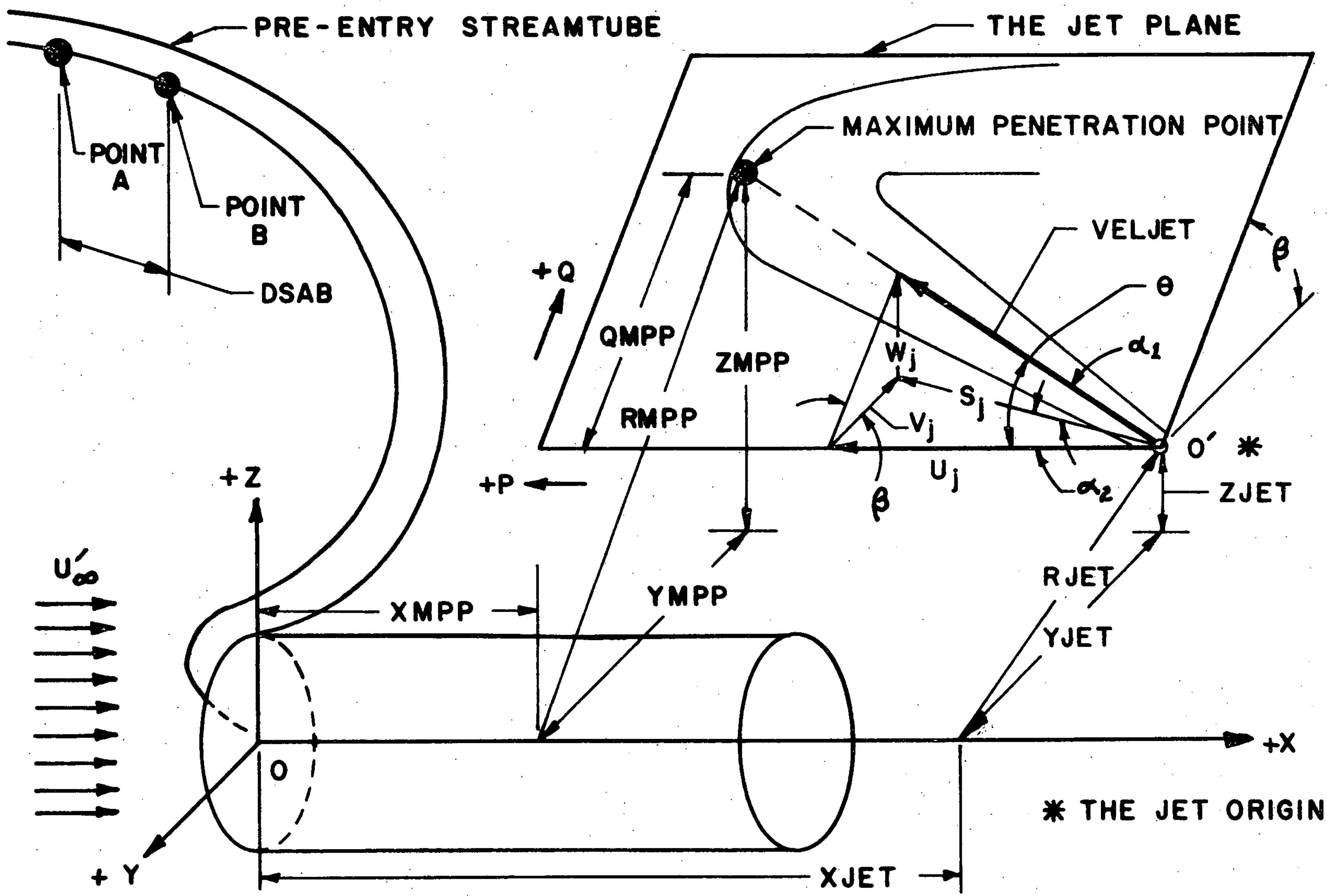

FIGURE 3. THE REVERSED JET

As the figure shows, the axisymmetric coordinate system of the inlet flow field model has been superimposed with a three-dimensional Cartesian system having the same origin. This new system is used to properly locate the origin of the jet plane with respect to the engine inlet. The angle between the freestream and the jet efflux in the P-Q coordinate system (θ) is defined in terms of the pitch angle ($\alpha 1$) and turning angle ($\alpha 2$). The P-Q coordinates of the Maximum Penetration Point are found from the Lockheed correlation. Then, a multiple transformation of coordinates is employed to establish the axial and radial coordinates of the Maximum Penetration Point with respect to the original axisymmetric coordinate system. This completes the reversed jet flow field model.

The geometries of the two flow fields are now superimposed to evaluate the likelihood of reingestion. If reingestion is predicted, the computer program is designed to note this and to determine the approximate time required for a fluid particle to travel from the Maximum Penetration Point to the engine inlet.

CHAPTER IV

DEVELOPMENT OF THE MATHEMATICAL MODEL

The Initial Singularity Strengths

Before developing the inlet flow field model, it is useful to determine the initial compensatory singularity strength used in the iterative nacelle generation procedure.

Consider an isolated area A' containing a singularity of strength $\dot{m}'$. The volumetric flowrate Q' associated with this surface can be expressed as:

$$Q' = \dot{m}'A'g'$$

where g' is the number of singularities per unit area and is equal to one in this case. In general, however, volumetric flowrate can be expressed as the product of a flow area and the velocity (V_n') normal to it. For a singularity, the flow area is twice the area in the above equation because fluid simultaneously enters or leaves both sides. Hence:

$$Q' = 2A' \cdot V_n'$$

Combining the two equations gives the singularity strength as a function of V'_n , or:

$$\dot{m}' = 2V'_n \text{ (for } g' = 1) \tag{1}$$

Therefore, the initial step in the iterative procedure is to set the strength of each singularity equal to twice the negative of the normal velocity induced by the freestream-inlet combination at the point to produce the cancelling normal velocity, V'_n .

The Inlet Flow Field Model

Let P in Figure 4 represent an arbitrary point in the flow field. The velocity potential induced at point P by all of the elements of the model can be described from potential flow theory as:

$$\varphi' = \varphi'_{FS} + \varphi'_S + \varphi'_{CR} + \varphi'_{CAX} \tag{2a}$$

where the terms on the right of the above expression represent the contributions to the potential from the freestream, the inlet sink, the distributed singularities on the nacelle, and the distributed singularities on the end cap, respectively.

It is convenient to work with non-dimensional terms. Towards this end, length terms are non-dimensionalized with respect to the nacelle radius R', while velocity terms are divided by the freestream velocity U'_∞. The velocity potential terms are made dimensionless by

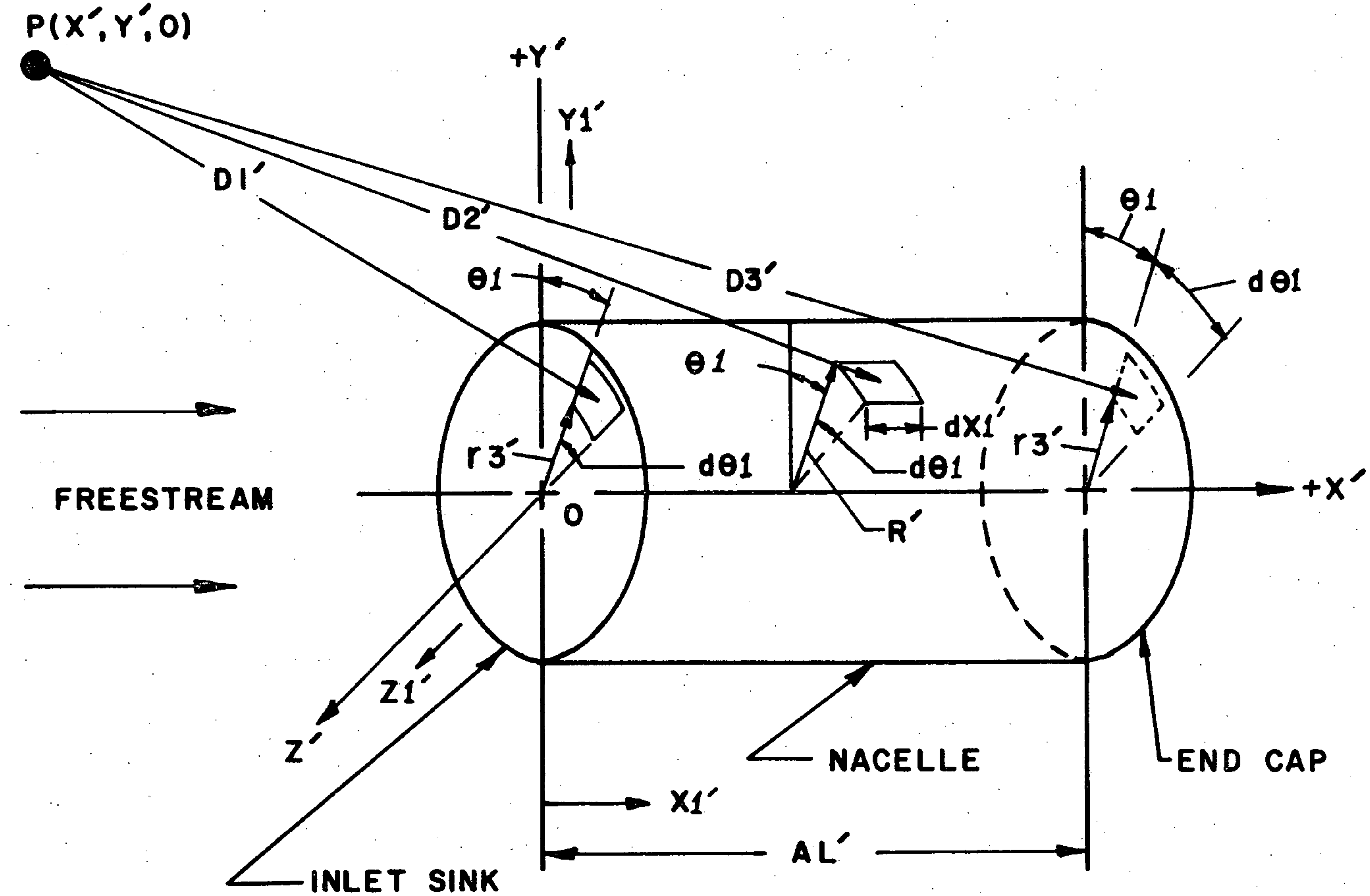

FIGURE 4. THE INLET FLOW FIELD MODEL

referring them to the product of the freestream velocity and nacelle radius. Equation 2a can thus be rewritten:

$$\varphi = \frac{\varphi'}{U'_\infty R'} = \varphi_{FS} + \varphi_S + \varphi_{CR} + \varphi_{CAX} \tag{2b}$$

It is also convenient to group ther terms associated with the freestream and inlet sink together, or:

$$\varphi 1 = \varphi_{FS} + \varphi_S \tag{3}$$

Hence, equation 2b becomes:

$$\varphi = \varphi 1 + \varphi_{CR} + \varphi_{CAX} \tag{4}$$

From potential flow theory, the radial and axial velocities at a point can be determined by taking the appropriate partial derivatives of equation 4; e.g.

$$\text{VRAD} = \frac{\partial \varphi}{\partial r} = \frac{\partial \varphi 1}{\partial r} + \frac{\partial \varphi_{CR}}{\partial r} + \frac{\partial \varphi_{CAX}}{\partial r} \tag{5}$$

and

$$\text{VAXY} = \frac{\partial \varphi}{\partial x} = \frac{\partial \varphi 1}{\partial x} + \frac{\partial \varphi_{CR}}{\partial x} + \frac{\partial \varphi_{CAX}}{\partial x} \tag{6}$$

The four velocity potential terms in equation 2b are now to be developed. From potential flow theory, a freestream can be described as:

$$\varphi'_{FS} = U'_{\infty} x'$$

or in non-dimensional terms:

$$\varphi_{FS} = x \tag{7}$$

The remaining terms in equation 2b describe surfaces of distributed singularities. Figure 5 shows an arbitrary surface divided into subareas dA', each containing one singularity of strength $\dot{m}'$. The incremental velocity potential induced at a point P by any such subarea, a distance D' away can be described by [13]:

$$d\varphi' = \frac{1}{4\pi} \frac{\dot{m}' dA'}{D'}$$

Hence, the velocity potential induced at P by all such subareas can be written as:

$$\varphi' = \frac{1}{4\pi} \int_A \frac{\dot{m}' dA'}{D'}$$

or in non-dimensional form:

$$\varphi = \frac{1}{4\pi U'_{\infty} R'} \int_A \frac{\dot{m}' dA'}{D'} \tag{8}$$

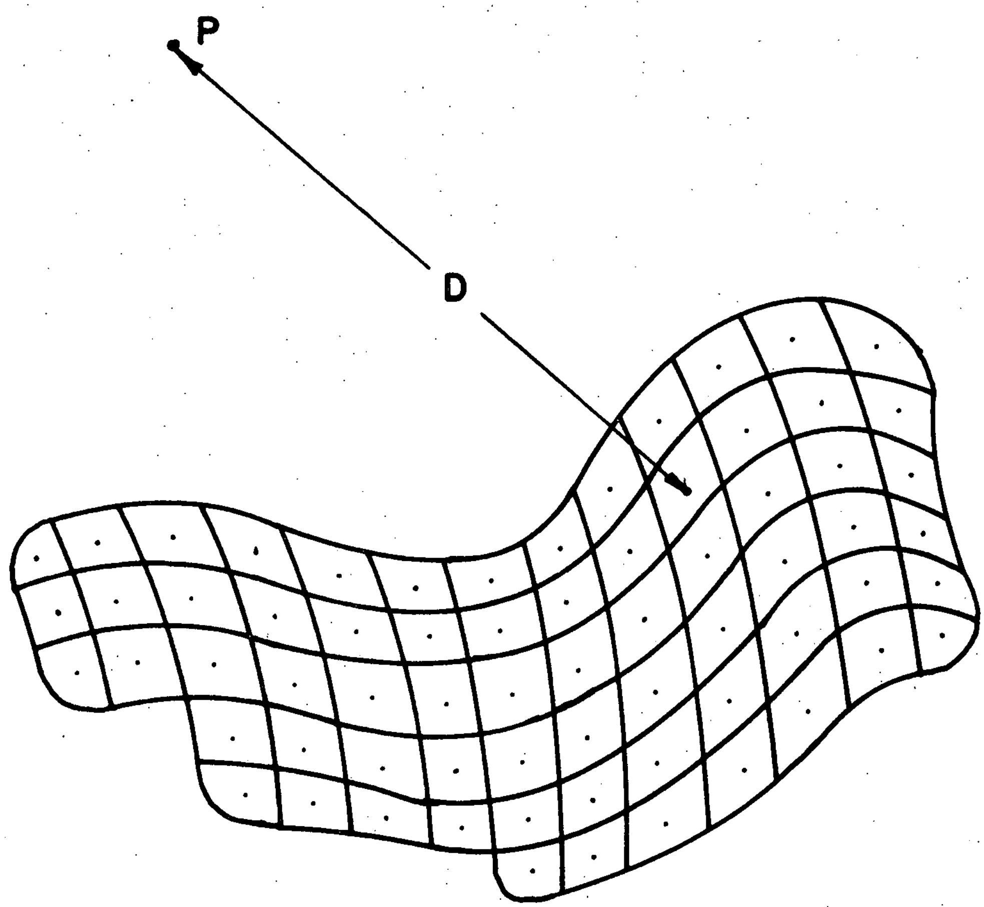

FIGURE 5. ARBITRARY SURFACE WITH DISTRIBUTED SINGULARITIES

If, in Figure 5, point P lies on the surface, then the subarea containing P must be excluded from the integration of equation 8.

Two of the components of the model to be described by equation 8 are disks. Hence as Figure 4 shows the area integral in equation 8 is evaluated with respect to r3' and θ1 and can be written:

$$dA' = r3'\ dr3'\ d\theta 1$$

or

$$dA' = (R')^2\ r3\ dr3\ d\theta 1 \tag{9}$$

The remaining component to be described by equation 8 is the cylinder and hence the area integral is evaluated with respect to **x1'** and θ1; or:

$$dA' = R'\ dx1'\ d\theta 1$$

or

$$dA' = (R')^2\ dx1\ d\theta 1 \tag{10}$$

With continuing reference to equation 8, Figure 4 shows that there are three D' terms: one for the inlet (D1'), one for the cylinder (D2') and one for the end cap (D3'). In general, the distance between point P and any point on the nacelle can be written:

$$D' = \sqrt{(x'-x1')^2 + (y'-y1')^2 + (z' - z1')^2}$$

or

$$D' = (R')\sqrt{(x-x1)^2 + (y-y1)^2 + (z - z1)^2} \tag{11}$$

The terms x, y, and z, are the coordinates of point P from the origin. The terms x1, y1, and z1, are the coordinates of any point on the nacelle. Because the system under study is axisymmetric, reference point P can be defined as always lying at z = 0.

In evaluating the D1' and D3' expressions, the areas involved are disks and hence the x1 terms are zero for the former and AL for the latter. In all the D' expressions, the values of y1 and z1 can be written:

$$z1 = r3 \sin \theta$$

and

$$y1 = r3 \cos \theta$$

In the D1' and D3' expressions, r3 terms in the above pair of equations remain as variables while in the D2' expression r3 is a constant with a value of unity. The three distance equations can thus be written, after simplification, as:

$$D1' = (R')\sqrt{x^2 + r^2 - 2r\, r3 \cos \theta 1 + r3^2} \tag{12}$$

$$D2' = (R')\sqrt{(x-x1)^2 + r^2 - 2r \cos \theta 1 + 1} \tag{13}$$

and

$$D3' = (R')\sqrt{(x-AL)^2 + r^2 - 2r\, r3 \cos \theta 1 + r3^2} \tag{14}$$

The remaining term to be considered in equation 8 is the singularity strength, $\dot{m}'$. For the case of the inlet sink, the strength (qs1') is constant over the area and is a function of a particular engine design and/or engine power setting. Thus it can be brought outside the integral.

In the cases of the nacelle and end cap surfaces, $\dot{m}'$ is a function of axial position along the nacelle and radial position along the end cap. Therefore in these cases $\dot{m}'$ must remain inside the integrals. As mentioned in the previous section, the strength of each singularity on these surfaces is initially set at twice the negative of the normal velocity induced by the freestream-inlet combination at the point.

All of the expressions necessary to describe the velocity potential at an arbitrary point can now be written. Combining equations 7, 8, 9, and 12 with equation 3 gives, after simplification, the potential due to the freestream and inlet:

$$\varphi 1 = x + \frac{qs1}{4\pi} \int_{o}^{2\pi} \int_{o}^{1} \frac{r3\ dr3\ d\theta 1}{[x^2 + r^2 - 2r\ r3 \cos\ \theta 1 + r3^2]^{1/2}} \qquad (15)$$

where the limits of integration in this and all of the velocity potential expressions are those already noted for the surface areas under consideration.

An expression for the potential due to the nacelle can be obtained by combining equations 1, 8, 10, and 13 and gives, after simplification:

$$\varphi_{CR} = \frac{1}{2\pi} \int_0^{2\pi} \int_0^{AI} \frac{Vr(x1)\ dx1\ d\theta 1}{[(x-x1)^2 + r^2 - 2r \cos\ \theta 1 + 1]^{1/2}} \qquad (16)$$

And finally, combining equations 1, 8, 9, and 14 gives, upon simplification, the potential due to the end cap:

$$\varphi_{CAX} = \frac{1}{2\pi} \int_0^{2\pi} \int_0^{1} \frac{VAX\ (r3)\ r3\ dr3\ d\theta 1}{[(x-AL)^2 + r^2 - 2r\ r3 \cos\ \theta 1 + r3^2]^{1/2}} \qquad (17)$$

In order to evaluate equations 5 and 6 the partial derivatives of the above three equations must be taken with respect to x and r. Applying Leibnitz's rule [14] to equations 15, 16, and 17 gives, upon simplification:

$$\frac{\partial \varphi 1}{\partial r} = -\frac{qs1}{4\pi} \int_0^{2\pi} \int_0^{1} \frac{(r - r3 \cos\ \theta 1)\ r3\ dr3\ d\theta 1}{[x^2 + r^2 - 2r\ r3 \cos\ \theta 1 + r3^2]^{3/2}} \qquad (18)$$

$$\frac{\partial \varphi_{CR}}{\partial r} = -\frac{1}{2\pi} \int_0^{2\pi} \int_0^{AL} \frac{[Vr\ (x1)][r - \cos\ \theta 1]\ dx1\ d\theta 1}{[(x-x1)^2 + r^2 - 2r \cos\ \theta 1 + 1]^{3/2}} \qquad (19)$$

$$\frac{\partial \varphi_{CAX}}{\partial r} = -\frac{1}{2\pi} \int_0^{2\pi} \int_0^{1} \frac{[VAX\ (r3)][r - r3 \cos\ \theta 1][r3]\ dr3\ d\theta 1}{[(x-AL)^2 + r^2 - 2r\ r3 \cos\ \theta 1 + r3^2]^{3/2}} \qquad (20)$$

$$\frac{\partial \varphi 1}{\partial x} = 1 - \frac{qs1 \cdot x}{4\pi} \int_0^{2\pi} \int_0^{1} \frac{r3\ dr3\ d\theta 1}{[x^2 + r^2 - 2r\ r3 \cos\ \theta 1 + r3^2]^{3/2}} \qquad (21)$$

$$\frac{\partial \varphi_{CR}}{\partial x} = -\frac{1}{2\pi}\int_0^{2\pi}\int_0^{AL} \frac{[Vr\ (x1)][x-x1]\ dx1\ d\theta 1}{[(x-x1)^2 + r^2 - 2r\cos\ \theta 1 + 1]^{3/2}} \tag{22}$$

$$\frac{\partial \varphi_{CAX}}{\partial x} = -\frac{1}{2\pi}\int_0^{2\pi}\int_0^{1} \frac{[VAX\ (r3)][x-AL][r3]\ dr3\ d\theta 1}{[(x-AL)^2 + r^2 - 2r\ r3\cos\ \theta 1 + r3^2]^{3/2}} \tag{23}$$

The above equations must be integrated to obtain the six velocity components. Integrations involving both variables of equations 19, 20, 22, and 23 must be performed numerically because of the dependence of the singularity strengths on position. Equations 18 and 21, however, can be integrated in closed form with respect to r3, though they must be integrated numerically with respect to $\theta 1$. Performing the cosed form integration gives:

$$\frac{\partial \varphi 1}{\partial r} = -\frac{qs1}{4\pi}\int_0^{2\pi}\left\{\left(\frac{r}{4A-B^2}\right)\left[4\sqrt{A} - \frac{(2B+4A)}{\sqrt{A+B+1}}\right]\right.$$

$$- \cos\ \theta 1\left\{\left(\frac{1}{4A-B^2}\right)\left(\frac{2B^2 - 4A + 2AB}{\sqrt{A+B+1}} - 2B\sqrt{A}\right)\right.$$

$$\left.\left. + \ell n\left[\frac{\sqrt{A+B+1} + B/2 + 1}{\sqrt{A} + B/2}\right]\right\}\right\} d\theta 1 \tag{24}$$

and

$$\frac{\partial \varphi 1}{\partial x} = 1 - \frac{qs1 \cdot x}{4\pi} \int_{o}^{2\pi} \left(\frac{1}{4A+B^2} \right) \left[4\sqrt{A} - \frac{(2B + 4A)}{\sqrt{A + B + 1}} \right] d\theta 1 \qquad (25)$$

where $\quad A = x^2 + r^2 \qquad (26)$

and $\quad B = -2r \cos \theta 1 \qquad (27)$

Numerical results using equations 5 and 6 can be obtained when the singularity strengths have been evaluated.

Evaluation of the Singularity Strengths - The Iterative Procedure

To satisfy the no-flow condition the normal velocity must vanish at each nacelle and end cap singularity. As explained earlier, the first step toward this end is to set the singularity strength at each location equal to twice the negative of the normal velocity induced by the free-stream-inlet combination. Consider any point P on the nacelle surface. The normal velocity CHEKR at P is determined from the equation:

$$\text{CHEKR} = \left. \frac{\partial \varphi 1}{\partial r} - Vr + \frac{\partial \varphi_{CR}}{\partial r} + \frac{\partial \varphi_{CAX}}{\partial r} \right|_{\text{at P}} \qquad (28)$$

In the above equation, the quantity Vr represents the velocity produced by the singularity at P and is initially equal in magnitude to $\frac{\partial \varphi 1}{\partial r}$. The remaining terms are identical to the corresponding terms in equation 5. However, because point P lies on the nacelle surface, the area containing P must be excluded from the numerical integration of the $\frac{\partial \varphi_{CR}}{\partial r}$ term (equation 19).

The no-flow boundary condition is satisfied along the nacelle when the velocity CHEKR vanishes at each singular point.

An equation analogous to equation 28 for the normal velocity at any point P on the end cap is:

$$CHEKX = \frac{\partial \varphi 1}{\partial x} - VAX + \frac{\partial \varphi_{CR}}{\partial x} + \frac{\partial \varphi_{CAX}}{\partial x} \Bigg|_{\text{at } P} \tag{29}$$

The partial differential terms in the above equation are identical to the corresponding terms in equation 6. The quantity VAX represents the velocity produced by the singularity at P and is initially equal in magnitude to $\frac{\partial \varphi 1}{\partial x}$. In performing the numerical integration of the $\frac{\partial \varphi_{CAX}}{\partial x}$ term, the area containing P must be excluded.

The no-flow boundary condition is satisfied along the end cap when the velocity CHEKX vanishes at each singular point.

The iterative procedure used in generating the nacelle and end cap surfaces is as follows:

1. The normal velocity induced by the freestream-inlet combination is calculated at each nacelle $\left(\frac{\partial \varphi 1}{\partial r}\right)$ and end cap $\left(\frac{\partial \varphi 1}{\partial x}\right)$ singular point by evaluating equations 24 and 25, respectively.

2. At each nacelle singular point, Vr is set equal to the negative of $\frac{\partial \varphi 1}{\partial r}$, while at each end cap singular point, VAX is set equal to the negative of $\frac{\partial \varphi 1}{\partial x}$.
3. The normal velocity CHEKR is determined at each nacelle singular point by evaluating equation 28 and the normal velocity CHEKX is determined at each end cap singular point by evaluating equation 29.
4. At each nacelle singular point where CHEKR is non-zero, an adjustment scheme (to be described below) resets Vr. Likewise, at each end cap singular point where CHEKX is non-zero, VAX is reset.
5. The procedure is repeated from STEP 3 until the no-flow condition is met at all singular points to some specified precision.

The adjustment procedure mentioned in STEP 4 is as follows. Consider first equation 28. Figure 6 represents all of the velocity components associated with this equation for a singular point P on the nacelle surface. Let it be assumed that CHEKR at P is not zero and hence Vr must be adjusted. The first step is to determine if

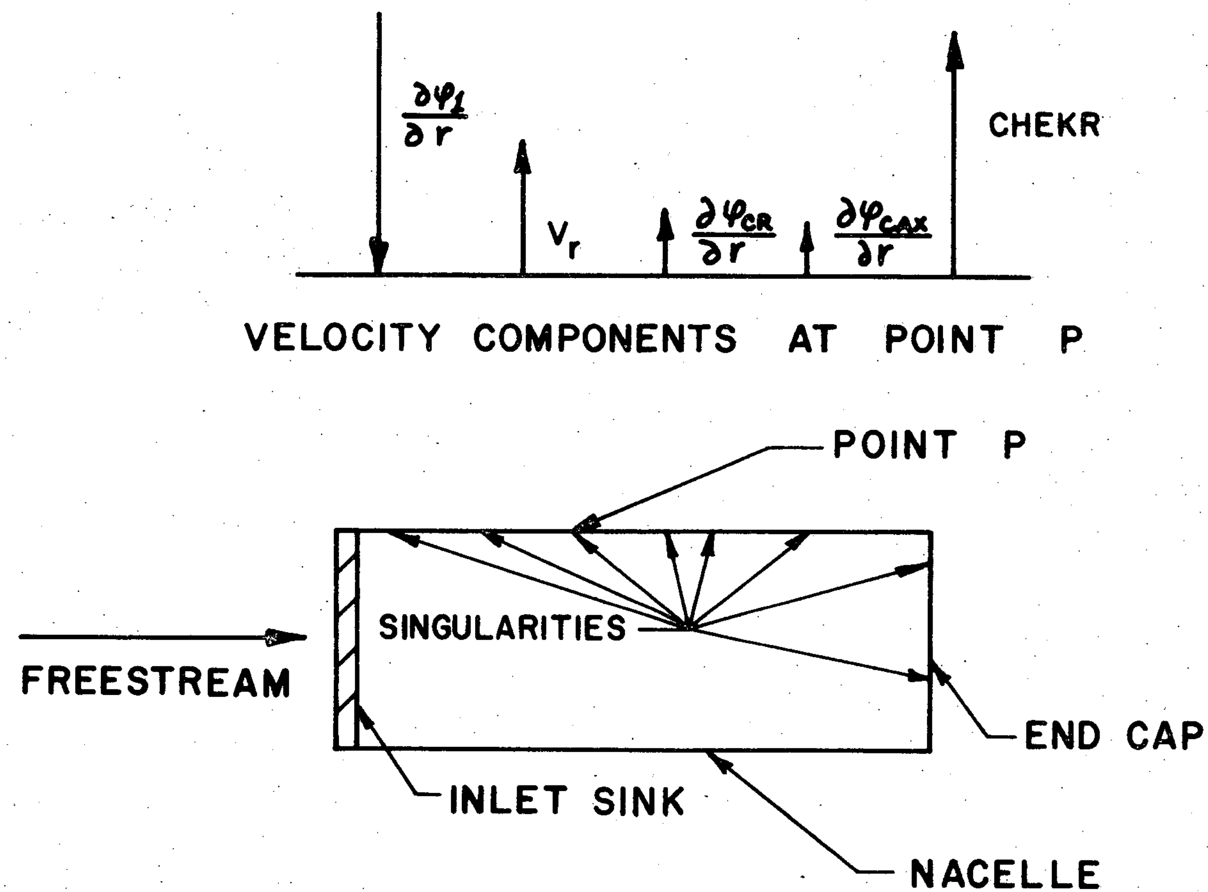

FIGURE 6. SINGULAR POINT VELOCITY VECTORS

CHEKR and Vr are of the same sign. If they are not, the magnitude of Vr must be increased. This is done by employing the equation:

$$Vr\Big|_{new} = Vr\Big|_{old} - CHEKR/2 \tag{30}$$

The choice of the correction term, CHEKR/2, in equation 30 is arbitrary.

If Vr and CHEKR are of opposite sign, the magnitude of Vr must be decreased. The procedure for doing this depends on the value of CHEKR/2. If the magnitude of CHEKR/2 is less than that of Vr, equation 30 is applied. However, if the magntide of CHEKR/2 is greater than that of Vr, the new Vr is obtained from:

$$Vr\Big|_{new} = Vr\Big|_{old} \Big/ 2.00 \tag{31}$$

Again, the choice of the correction is arbitrary.

An identical adjustment procedure is used along the end cap with CHEKX (from equation 29) substituted for CHEKR and VAX substituted for Vr in equations 30 and 31.

Generation of the Streamlines

Let a fluid particle be released from a point P in the flow field with the object being to determine the path it follows. Since the flow field is assumed to be in equilibrium, the fluid particle will travel along a streamline. The value of the stream function along any streamline is constant and hence:

$$\partial\Psi = 0 \Big|_{\text{Along any streamline}} \qquad (32)$$

In an axisymmetric system, the stream function is a function of x and r and hence:

$$\Psi = \Psi(x,r)$$

Taking the derivative and applying it along a streamline gives:

$$\partial\Psi = 0 = \frac{\partial\Psi}{\partial r}\, dr + \frac{\partial\Psi}{\partial x}\, dx$$

or rearranging:

$$\left.\frac{dr}{dx}\right|_{\Psi = \text{Const.}} = -\frac{\partial\Psi/\partial x}{\partial\Psi/\partial r} \qquad (33)$$

The radial and axial velocity at any point in an axisymmetric system can be expressed from Stokes Stream Function [15] as:

$$VAXY = \frac{1}{r}\frac{\partial\Psi}{\partial r}$$

and

$$VRAD = -\frac{1}{r}\frac{\partial\Psi}{\partial x}$$

Rearranging the above two equations and combining them with equation 33 gives, after simplification:

$$\left.\frac{dr}{dx}\right|_{\Psi = \text{Const.}} = \frac{VRAD}{VAXY} \qquad (34)$$

With the coordinates of the release point known, the above differential equation can be numerically solved using the Runge-Kutta Method [16] to determine the radial and axial coordinates of the points along the streamline which the fluid particle follows. The velocities VRAD and VAXY needed in this solution are obtained by evaluating equations 5 and 6, respectively.

The Reversed Jet Flow Field Model

This section developes the axial and radial coordinates of the Maximum Penetration Point of the reversed jet relative to the axisymmetric coordinate system of the inlet flow field model. The problem is defined in Figure 3.

The P coordinate of the Maximum Penetration Point in the jet plane is found from the Lockheed correlation (Figure 1):

$$\mathrm{PMPP} = 2.97\ (\mathrm{DIAJET})(\mathrm{VELJET})^{.94}(1 - .734\mathrm{SIN}^{.685}\theta) \quad (35)$$

From Figure 3, the Q coordinate of the Maximum Penetration Point can be written:

$$\mathrm{QMPP} = \mathrm{PMPP}\ \tan\ \theta \quad (36)$$

The axial coordinate of the Maximum Penetration Point with respect to the axisymmetric coordinate system can be written from Figure 3 as:

$$\mathrm{XMPP} = \mathrm{XJET} - \mathrm{PMPP} \quad (37)$$

where PMPP is found from equation 35. An expression must now be developed for the radial coordinate of the Maximum Penetraion Point with respect to the axisymmetric coordinate system. From Figure 3:

$$\mathrm{RMPP} = \sqrt{\mathrm{YMPP}^2 + \mathrm{ZMPP}^2} \tag{38}$$

where:

$$\mathrm{YMPP} = \mathrm{YJET} + \mathrm{QMPP} \cdot \cos(\beta)$$

and

$$\mathrm{ZMPP} = \mathrm{ZJET} + \mathrm{QMPP} \cdot \sin(\beta)$$

Substituting the above expressions into equation 38 gives, upon simplification:

$$\mathrm{RMPP} = \sqrt{\mathrm{YJET}^2 + \mathrm{ZJET}^2 + 2\ \mathrm{QMPP}\ [\mathrm{YJET}\cdot\cos\beta + \mathrm{ZJET}\cdot\sin\beta] + \mathrm{QMPP}^2} \tag{39}$$

Everything necessary to solve equation 39 has now been developed except for the in-plane angles, θ and β. From Figure 3:

$$s_J = \mathrm{VELJET} \cdot \cos \alpha 1$$

or:

$$\frac{s_J}{\mathrm{VELJET}} = \cos \alpha 1 \tag{40}$$

Likewise, for u_J

$$u_J = s_J \cos \alpha 2$$

or:

$$\frac{u_J}{s_J} = \cos \alpha 2 \tag{41}$$

From Figure 3:

$$\cos\theta = u_J/VELJET \tag{42}$$

Equation 42 can be rearranged as:

$$\cos\theta = \frac{s_J}{VELJET} \cdot \frac{u_J}{s_J}$$

Combining equations 40 and 41 with the above gives:

$$\cos\theta = \cos\alpha 1 \cdot \cos\alpha 2$$

or:

$$\theta = \cos^{-1}[\cos\alpha 1 \cdot \cos\alpha 2] \tag{43}$$

Referring to Figure 3, the following can be written:

$$\tan\alpha 1 = w_J/s_J \tag{44}$$

and

$$\sin\alpha 2 = v_J/s_J \tag{45}$$

Also,

$$\tan\beta = w_J/v_J \tag{46}$$

Equation 46 can be rearranged as:

$$\tan\beta = \frac{w_J}{s_J} \cdot \frac{s_J}{v_J}$$

Combining equations 44 and 45 with the above gives:

$$\tan \beta = \tan \alpha 1 / \sin \alpha 2$$

or:

$$\beta = \mathrm{TAN}^{-1} \left[\frac{\mathrm{TAN}\ \alpha 1}{\sin\ \alpha 2} \right] \tag{47}$$

With equations 43 and 47 complete, the location of the Maximum Penetration Point with respect to the axisymmetric coordinate system can be determined from equations 37 and 39.

Time Calculations

This section develops a method of approximating the time required for a fluid particle to travel from the Maximum Penetration Point to the engine inlet, for cases where reingestion occurs. Figure 3 shows two points, A and B, on a streamline located within the pre-entry streamtube. Equations have already been developed for finding both the radial and axial velocitites at these points (equations 5 and 6), as well as the locations of the points themselves, (equation 34). Let the quantity VAB be defined as the average speed between points A and B. It follows then, that:

$$\mathrm{VAB} = \frac{\mathrm{VPA} + \mathrm{VPB}}{2} \tag{48}$$

where VPA and VPB are the speeds at points A and B, respectively. These speeds can be determined from:

$$\mathrm{VP} = \sqrt{(\mathrm{VAXY})^2 + (\mathrm{VRAD})^2} \tag{49}$$

Let XAB be the axial distance between the points and RAB be the radial distance between the points. Then:

$$XAB = XA - XB \tag{50a}$$

and

$$RAB = RA - RB \tag{50b}$$

The approximate distance between the points, DSAB can be described as:

$$DSAB = \sqrt{(XAB)^2 + (RAB)^2} \tag{51}$$

From the elementary equation, distance equals speed times time, DSAB can also be expressed as:

$$DSAB = (VAB)(TAB)$$

where TAB is the time required for the particle to travel the distance DSAB at an average speed of VAB. The above equation can be rewritten as:

$$TAB = \frac{DSAB}{VAB} \tag{52}$$

By summing the TAB values between all of the points along the streamline from the Maximum Penetration Point to the inlet, the approximate time involved in the reingestion process can be determined.

Cross Ingestion

Figure 7 shows a sketch of a four-engined jet transport with wing-mounted engines. The quantities XOP and RCROSS are defined

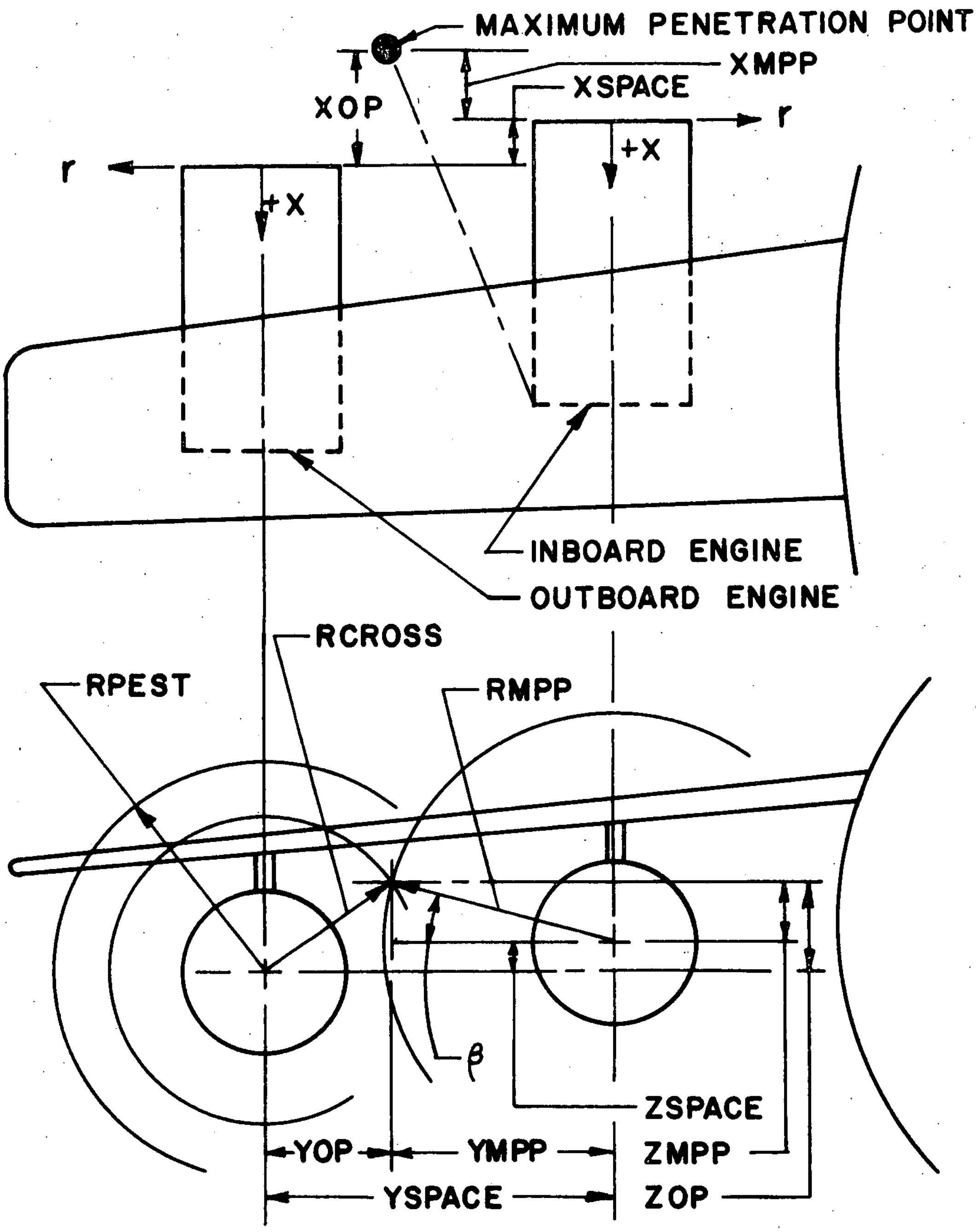

FIGURE 7. THE CROSS INGESTION MODEL

respectively as the axial and radial coordinates of the Maximum Penetration Point of the reversed jet of the inboard engine relative to the outboard engine coordinate system. Clearly cross ingestion occurs if RCROSS lies within the outboard engine pre-entry streamtube at XOP. With this in mind, expressions for these quantities are now developed.

The first step is to establish the center point of the inboard engine end cap relative to the same point on the outboard engine with the quantities XSPACE, YSPACE, and ZSPACE. With this done, XOP can be described as:

$$XOP = XMPP - XSPACE \tag{53}$$

From Figure 7, the following expressions can also be written:

$$YOP = YSPACE - YMPP \tag{54}$$

and

$$ZOP = ZSPACE + ZMPP \tag{55}$$

From these two equations, RCROSS can be described as:

$$RCROSS = \sqrt{YOP^2 + ZOP^2} \tag{56}$$

With XOP and RCROSS determined, the likelihood of cross ingestion can be evaluated.

The Pre-entry Streamtube Radius Equation

The most important streamtube is the pre-entry streamtube and while the radius of this boundary cannot be analytically determined at arbitrary axial locations, it can be determined at minus infinity (RPEST). At minus infinity, the velocity within the pre-entry streamtube is the freestream velocity $\left(\frac{U'_\infty}{U'_\infty} = 1\right)$. At the engine inlet, the velocity within the pre-entry streamtube is the sum of the freestream and inlet induced (VELRAT) velocities. The flow areas at these two axial locations are $\pi \cdot \mathrm{RPEST}^2$ and $\pi \cdot 1^2$, respectively. Since continuity is maintained within the pre-entry streamtube, the following can be written:

$$V \cdot A\Big|_{\text{at } -\infty} = V \cdot A\Big|_{\text{at Inlet}}$$

$$1 \cdot \pi \mathrm{RPEST}^2 = (\mathrm{VELRAT} + 1)\, \pi \cdot 1^2$$

or:

$$\mathrm{RPEST} = \sqrt{\mathrm{VELRAT} + 1} \tag{57}$$

CHAPTER V

THE COMPUTER PROGRAM

The statement listing of the computer program is presented in Appendix I. The block diagram of this program is shown in Figure 8 and for clarity, the step numbers in the figure are included in the statement listing.

Referring to Figure 8, the initial step in the program is the inputting of the geometric, dynamic, and program variables and selection of the program options. The procedure for doing this is described in Appendix II.

Program initialization for the first inlet-to-freestream velocity ratio to be studied occurs in STEP 2.

In STEP 3, the normal velocities induced at each nacelle and end cap singularity by the freestream-inlet combination are computed from equations 24 and 25, respectively.[1] In addition, the initial strength settings of the compensatory singularities are assigned here.

The iterative nacelle generation procedure comprises STEPS 4, 5, and 6. In STEP 4, the induced normal velocities at each nacelle and end

---

[1] For programming convenience, the number of singularities on the nacelle and end cap are equal.

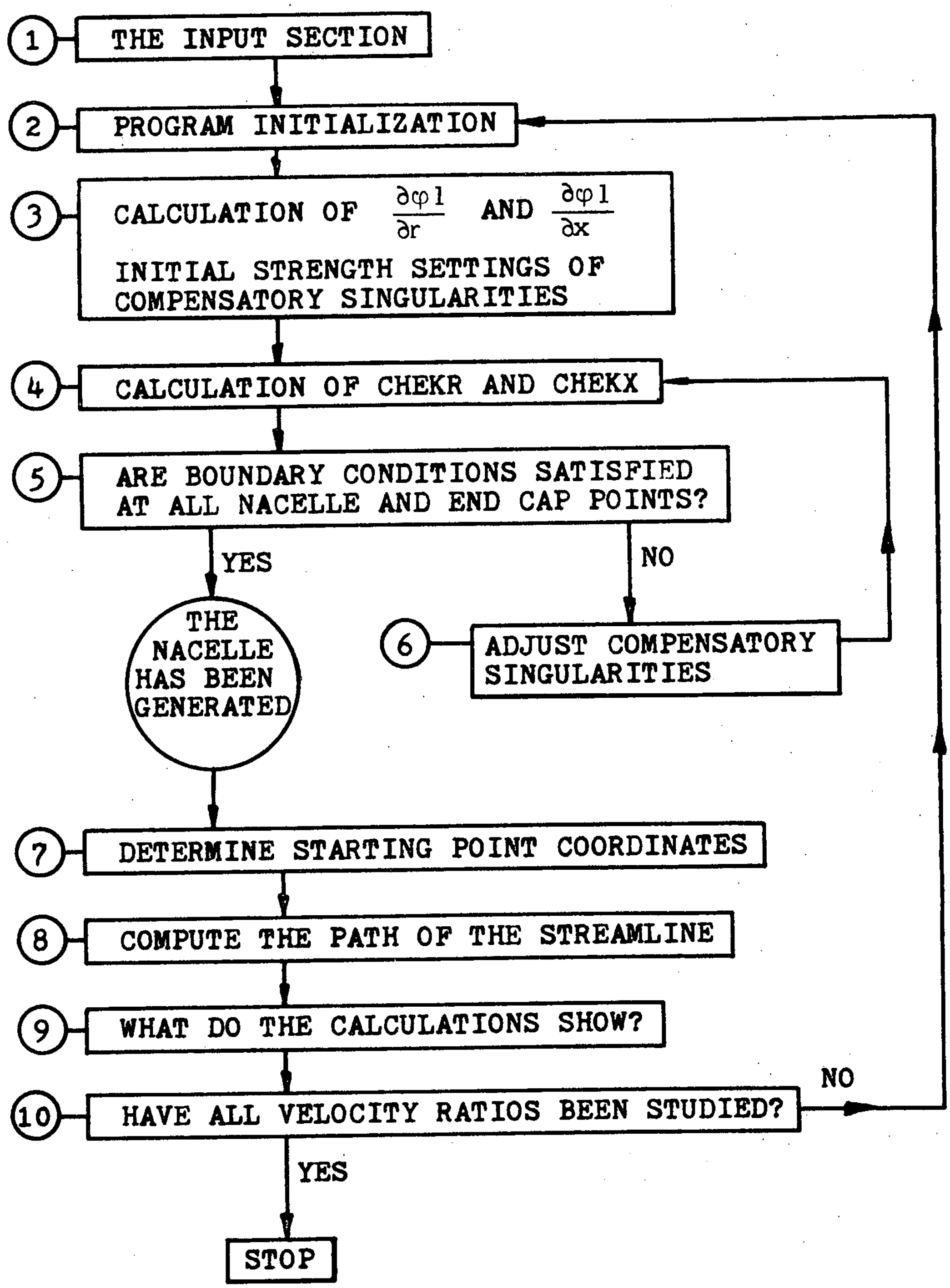

FIGURE 8. FLOW CHART OF THE COMPUTER PROGRAM

cap singularity due to all of the elements of the system are computed from equations 28 and 29, respectively. The purpose of STEP 5 is to record in computer memory those points where the above normal velocities have not vanished. At all such points the singularity strengths are adjusted in STEP 6 using the procedure described in Chapter IV. The degree of accuracy to which the no-flow condition is established is controlled by the inputted quantity EP, which represents a selected percentage of the freestream velocity.

The program proceeds to STEP 7 when the no-flow condition is met at every singular point. Otherwise, control is returned to STEP 4.

The purpose of STEP 7 is to provide the coordinates of a starting point for the streamline generation procedure of STEP 8. Two program options are available here. With one option the coordinates of the Maximum Penetration Point of the reversed jet are computed using the Lockheed correlation. This option is employed to evaluate the likelihood of reingestion. If the other option is chosen, the coordinates of an inputted point are used. This option is employed for generating selected streamlines.

With an initial point determined, the path of a streamline is generated in STEP 8. Additionally, the time required for a fluid particle to travel the streamline is determined here.

In STEP 9 the likelihood of reingestion is evaluated. Output confirms whether or not exhaust efflux has entered the engine inlet. If reingestion occurs, the fluid particle time is also outputted. Additionally, a program option is available to determine if the entraining portion of the jet penetrates the pre-entry streamtube.

Program operation is terminated in STEP 10 unless further inlet-to-freestream velocity ratios are to be studied. If this is the case, control is transferred back to STEP 2.

CHAPTER VI

RESULTS AND DISCUSSION

Varification of the operationality of the computer program consists of three steps:

1. Demonstration of the nacelle generation sections of the program. This is accomplished by showing that the inlet flow field model can be generated over a wide range of geometric and dynamic conditions, to any specified degree of accuracy.
2. Demonstration of the streamline computational scheme. This is accomplished qualitatively by plotting selected streamlines about a nacelle and quantitatively by showing that continuity is satisfied between adjacent streamlines.
3. Demonstration of the ability of the program to analyze a realistic reingestion problem.

Nacelle Generation

Results from several nacelle generation studies are presented in Tables 1 through 5. At each singularity, the tables note the normal

TABLE 1. NACELLE GENERATION DATA

VELRAT = 60; ASPECT RATIO = 3; EP = 0.01; NO. OF ITERATIONS = 12

Singularity Location	$\frac{\partial \varphi 1}{\partial r}$	Vr	CHEKR	$\frac{\partial \varphi 1}{\partial x}$	VAX	CHEKX
1	-29.12381	24.17546	0.007	0.18362	-0.75719	0.010
2	-25.46819	19.73041	0.005	.18371	- .75737	0.010
3	-14.12882	9.91636	0.003	.18396	- .75785	0.010
4	- 8.70776	4.58291	0.001	.18436	- .76371	0.005
5	- 5.66953	2.44176	-0.010	.18494	- .76497	0.005
6	- 3.84147	1.35647	-0.010	.18566	- .76272	0.010
7	- 2.69018	.78559	-0.009	.18656	- .76994	0.005
8	- 1.93872	.47825	-0.007	.18760	- .77259	0.006
9	- 1.43300	.30737	-0.005	.18879	- .77628	0.007
10	- 1.08323	.20862	-0.004	.19016	- .78017	0.008
11	- 0.83533	.14861	-0.004	.19168	- .78562	0.009
12	- .65568	.10929	-0.005	.19334	- .79736	0.005
13	- .52286	.09744	0.008	.19518	- .80610	0.006
14	- .42287	.08309	0.009	.19716	- .81636	0.008
15	- .34636	.07186	0.006	.19929	- .83018	0.010
16	- .28693	.06938	0.005	.20154	- .85308	0.007
17	- .24015	.07722	0.005	.20397	- .87755	0.008
18	- .20286	.08830	-0.008	.20653	- .91593	0.005
19	- .17282	.14561	-0.007	.20923	- .96087	0.008
20	- .14835	.29073	-0.008	.21207	-1.01060	0.010
21	- .13781	.50227	-0.007	.21354	-1.03314	0.005

TABLE 2. NACELLE GENERATION DATA

VELRAT = 10; ASPECT RATIO = 3; EP = 0.01; NO. OF ITERATIONS = 12

Singularity Location	$\frac{\partial \varphi 1}{\partial r}$	Vr	CHEKR	$\frac{\partial \varphi 1}{\partial x}$	VAX	CHEKX
1	-4.85397	4.03431	0.007	0.86394	-1.01892	0.007
2	-4.24470	3.29298	0.006	.86395	-1.01914	0.007
3	-2.35480	1.50842	0.007	.86399	-1.01982	0.007
4	-1.45129	0.76922	0.006	.86406	-1.02095	0.007
5	-0.94492	.40662	-0.003	.86416	-1.02260	0.007
6	- .64025	.22387	-0.006	.86428	-1.02412	0.008
7	- .44836	.12865	-0.006	.86443	-1.02690	0.009
8	- .32312	.07572	-0.008	.86460	-1.03038	0.009
9	- .23883	.04957	-0.006	.86480	-1.03468	0.010
10	- .18054	.03204	-0.008	.86503	-1.04505	0.006
11	- .13922	.02505	-0.005	.86528	-1.05205	0.006
12	- .10928	.01624	-0.009	.86556	-1.05957	0.008
13	- .08714	.01584	-0.007	.86586	-1.07019	0.009
14	- .07048	.01789	-0.004	.86619	-1.08857	0.005
15	- .05773	.02283	-0.002	.86655	-1.10572	0.006
16	- .04782	.03210	-0.001	.86692	-1.12854	0.008
17	- .04002	.04972	-0.002	.86733	-1.15886	0.009
18	- .03381	.07909	-0.010	.86776	-1.20559	0.007
19	- .02880	.16141	-0.006	.86820	-1.26252	0.009
20	- .02472	.35474	-0.009	.86868	-1.33049	0.005
21	- .02297	.63382	-0.008	.86892	-1.35254	0.006

TABLE 3. NACELLE GENERATION DATA

VELRAT = 5; ASPECT RATIO = 2; EP = 0.01; NO. OF ITERATIONS = 14

Singularity Location	$\frac{\partial \varphi 1}{\partial r}$	Vr	CHEKR	$\frac{\partial \varphi 1}{\partial x}$	VAX	CHEKX
1	-2.42699	2.00175	0.009	.85071	-1.01983	0.008
2	-2.74531	2.25474	0.009	.85075	-1.02006	0.008
3	-1.71072	1.22803	0.007	.85084	=1.02075	0.008
4	-1.17740	0.74237	0.004	.85099	-1.02192	0.008
5	-0.84646	.47211	0.005	.85121	-1.02360	0.009
6	- .62576	.30499	0.002	.85150	-1.02485	0.010
7	- .47246	.20102	-0.001	.85184	-1.03277	0.005
8	- .36304	.13840	0.001	.85224	-1.03664	0.006
9	- .28331	.09497	-0.002	.85271	-1.04080	0.007
10	- .22418	.06794	-0.004	.85323	-1.04632	0.008
11	- .17967	.05194	-0.005	.85381	-1.05296	0.009
12	- .14569	.04375	-0.005	.85445	-1.06194	0.010
13	- .11942	.04371	-0.002	.85514	-1.07872	0.006
14	- .09886	.04334	-0.006	.85589	-1.09307	0.008
15	- .08260	.05370	-0.006	.85669	-1.11731	0.005
16	- .06961	.06959	-0.010	.85754	-1.14520	0.007
17	- .05912	.10802	-0.005	.85844	-1.18936	0.005
18	- .05058	.16379	-0.008	.85939	-1.25380	0.008
19	- .04357	.27233	-0.006	.86039	-1.37106	0.007
20	- .03777	.51670	-0.009	.86143	-1.56440	0.005
21	- .03524	.91305	-0.010	.96197	-1.66026	0.007

TABLE 4. NACELLE GENERATION DATA

VELRAT = 5; ASPECT RATIO = 4; EP = 0.01; NO. OF ITERATIONS = 11

Singularity Location	$\frac{\partial \varphi 1}{\partial r}$	VR	CHEKR	$\frac{\partial \varphi 1}{\partial x}$	VAX	CHEKX
1	-2.42699	2.02620	0.008	.96139	-1.05643	0.007
2	-1.71072	1.25887	0.007	.96139	-1.05665	0.007
3	- .84646	.48609	0.006	.96140	-1.05732	0.007
4	- .47246	.21190	0.005	.96141	-1.05844	0.007
5	- .28331	.09349	-0.004	.96142	-1.06006	0.007
6	- .17967	.04307	-0.008	.96144	-1.06222	0.008
7	- .11942	.02236	-0.007	.96147	-1.06497	0.008
8	- .08260	.01461	-0.004	.96150	-1.06841	0.008
9	- .05912	.00929	-0.004	.96153	-1.07265	0.009
10	- .04357	.00198	-0.009	.96156	-1.07781	0.010
11	- .03293	.00170	-0.008	.96161	-1.08912	0.005
12	- .02543	.00245	-0.005	.96165	-1.09688	0.006
13	- .02001	.00400	-0.003	.96170	-1.10670	0.007
14	- .01601	.00644	0.000	.96176	-1.11870	0.008
15	- .01300	.01300	0.006	.96182	-1.13342	0.009
16	- .01069	.01624	0.005	.96188	-1.15675	0.005
17	- .00889	.02644	0.005	.96195	-1.17934	0.007
18	- .00747	.04486	-0.002	.96202	-1.20706	0.008
19	- .00633	.10096	-0.006	.96209	-1.23760	0.009
20	- .00541	.26865	-0.009	.96217	-1.26875	0.005
21	- .00502	.51886	-0.008	.96221	-1.27575	0.006

TABLE 5. EFFECTS OF NO-FLOW CRITERIA

VELRAT = 5; ASPECT RATIO = 3

		PART A EP = 0.01 NO. OF ITERATIONS = 12		PART B EP = 0.001 NO. OF ITERATIONS = 19	
Singularity Location	$\frac{\partial\varphi 1}{\partial r}$	CHEKR	Vr	Vr	CHEKR
1	-2.42699	0.008	2.02155	2.01511	0.001
3	-1.17740	0.004	0.75460	0.75191	0.000
5	-0.47246	-0.002	0.20368	0.20418	-0.001
7	-0.22418	-0.007	0.06212	0.06643	-0.001
9	-0.11942	-0.006	0.02430	0.02711	-0.000
11	-0.06961	-0.007	0.01053	0.01485	-0.000
13	-0.04357	-0.004	0.01048	0.01265	-0.000
15	-0.02886	-0.001	0.01927	0.01931	0.000
17	-0.02001	-0.001	0.04803	0.04780	0.000
19	-0.01440	-0.006	0.16279	0.16727	-0.001
21	-0.01148	-0.008	0.64707	0.65953	-0.001
Singularity Location	$\frac{\partial\varphi 1}{\partial x}$	CHEKX	VAX	VAX	CHEKX
1	0.93197	0.007	-1.04498	-1.05467	0.001
3	0.93200	0.007	-1.04589	-1.05567	0.001
5	0.93208	0.007	-1.04870	-1.05890	0.001
7	0.93221	0.009	-1.05307	-1.06466	0.001
9	0.93240	0.010	-1.06097	-1.07378	0.001
11	0.93264	0.006	-1.07857	-1.08830	0.001
13	0.93293	0.009	-1.09704	-1.10979	0.001
15	0.93327	0.006	-1.13314	-1.14448	0.001
17	0.93366	0.009	-1.18730	-1.20247	0.001
19	0.93410	0.009	-1.29298	-1.30950	0.001
21	0.93446	0.006	-1.38476	-1.40059	0.001

velocity induced by the freestream-inlet combination $\left(\frac{\partial\varphi 1}{\partial r} \text{ or } \frac{\partial\varphi 1}{\partial x}\right)$, the normal velocity induced by all of the elements of the system (CHEKR or CHEKX), the singularity-produced velocity (Vr or VAX), and the number of iterations required to achieve the no-flow condition.

The singularity location numbering scheme used in the tables is as follows. The equally spaced nacelle singularities begin with point 1 at the inlet plane and run axially to point 21 at the end cap plane. Similarly, the equally spaced end cap singularities begin with point 1 on the nacelle centerline and run radially to point 21 at the nacelle surface.

To establish the inlet flow field model, the nacelle generation procedure must reduce the normal velocities CHEKR and CHEKX along the nacelle and end cap, respectively, to an absolute value no greater than the no-flow criteria, EP. A comparison of these normal velocities to the selected value of EP (0.01) in Tables 1-5A clearly confirms the generality of this procedure with respect to the inlet-to-freestream velocity ratio (VELRAT) and the nacelle aspect ratio (AL'/2R').

The two cases presented in Tables 5A and 5B have identical dynamic and geometric conditions but differ by an order of magnitude in EP. Table 5B shows that increased accuracy is readily obtainable, but at the expense of additional iterations and consequently additional computer time.

At most of the singularity locations in Tables 1-5 the magnitude of the singularity-produced velocity (Vr or VAX) required to establish the no-flow condition differs substantially from that of the normal velocity induced by the freestream-inlet combination $\left(\frac{\partial\varphi 1}{\partial r} \text{ or } \frac{\partial\varphi 1}{\partial x}\right)$. This shows the importance of using a singularity strength adjustment scheme to generate accurately the inlet flow field model.

The Streamline Computational Scheme

A series of streamlines generated using the computer program are presented in Figures 9 and 10. The results in both figures were obtained with a nacelle aspect ratio of 3 and an EP of 0.01.

The streamlines in Figure 9 were computed at a constant inlet-to-freestream velocity ratio of 5. Curve 1 in this figure represents the pre-entry streamtube. Moving progressively outward from curve 1, curves 2, 3, and 4 exhibit the expected decreasing influence of the nacelle's presence.

Figure 10 shows three pre-entry streamtubes, computed at inlet-to-freestream velocity ratios of 5, 10, and 60. This figure illustrates the increasing probability of exhaust gas reingestion with decreasing aircraft speed, due to the larger size of the pre-entry streamtube.

An additional pre-entry streamtube was calculated using a 5/1 inlet-to-freestream velocity ratio but with a 2/1 nacelle aspect ratio. The points on this curve were indistinguishable from the 3/1 nacelle

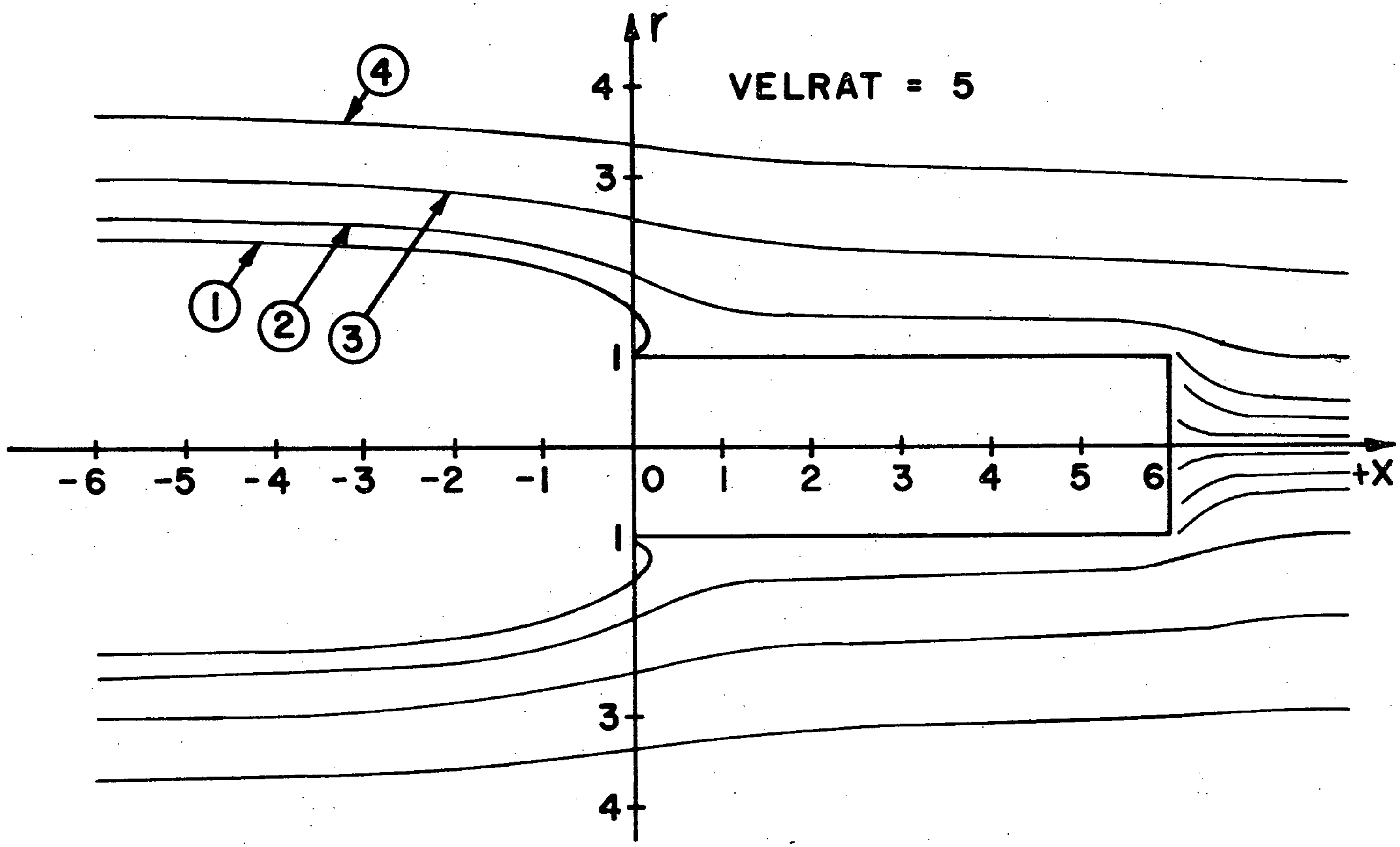

FIGURE 9. STREAMLINES ABOUT A NACELLE

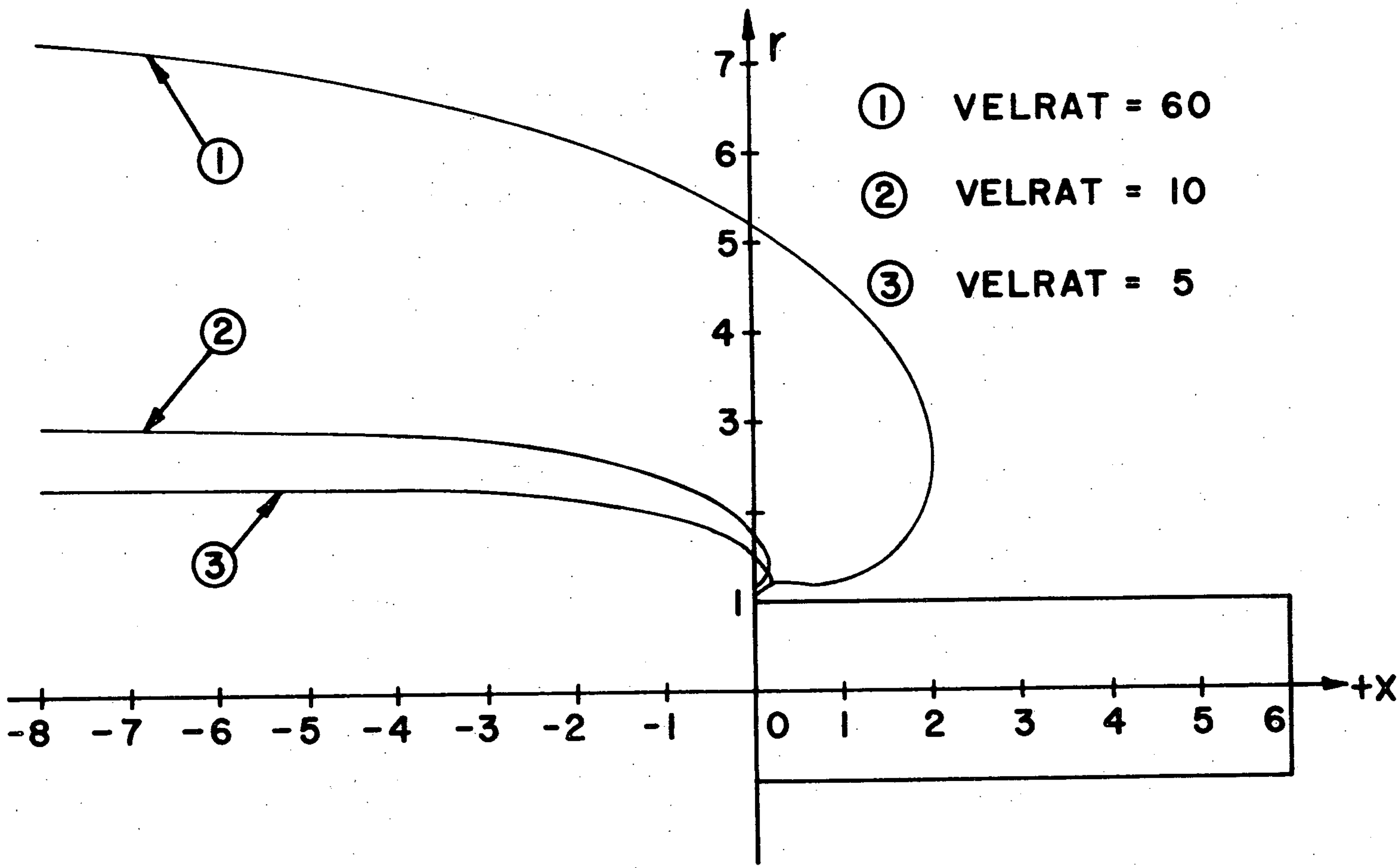

FIGURE 10. PRE-ENTRY STREAMTUBES

aspect ratio case. This suggests that the path of the pre-entry streamtube is not strongly dependent on the nacelle shape.

Table 6 presents the results of a check for continuity undertaken at three axial locations between several adjacent streamtubes in Figure 9. At each of the locations, the discharge (V·A) was found by summing the V·A products of 20 subareas. The results of the check show the discharge to be nearly constant between streamtubes. The maximum variation of only 1.2% from the average clearly demonstrates the precision of the streamline computational scheme.

TABLE 6. RESULTS OF CONTINUITY CHECK

AXIAL LOCATION	DISCHARGE (V·A) Between Streamtubes 2 & 3	DISCHARGE (V·A) Between Streamtubes 3 & 4
-5.100	$2.57115\ \pi$	$4.81250\ \pi$
3.000	$2.54358\ \pi$	$4.79576\ \pi$
8.850	$2.51183\ \pi$	$4.79334\ \pi$

The Reingestion Example

The dynamic and geometric conditions of the example problem are presented in Table 7. The example begins with the touchdown of a four-engined (wing-mounted) STOL transport and continues through the full deceleration process.

The results are included in Table 7 and Figure 11. In this example, deceleration for the inboard engine occurs reingestion free. Also, the entrainment portions of both reversed jets never penetrate the pre-entry streamtubes of the engines discharging them. The aircraft configuration, however, proves to be highly prone to cross ingestion of the inboard engine exhaust to the outboard engine. Cross ingestion begins at an aircraft speed of about 70 miles per hour and continues through 50 miles per hour. Below this speed, the Maximum Penetration Point of the reversed jet of the inboard engine lies outside of the inlet flow field of the outboard engine. The entraining portion of the jet, however, continues to lie in this flow field and thus the possibility of further cross ingestion remains.

Table 7 also lists the fluid particle time for those speeds where cross ingestion occurs.

TABLE 7. EXAMPLE PROBLEM

DYNAMIC AND GEOMETRIC CONDITIONS

VELJET'	=	880	Ft/Sec.
INLET VELOCITY	=	440	Ft/Sec.
R'	=	2.000	Ft.
AL'	=	22.6	Ft.
XJET'	=	20.	Ft.
YJET'	=	2.	Ft.
ZJET'	=	0.0	Ft.
XSPACE'	=	16.0	Ft.
YSPACE'	=	24.0	Ft.
ZSPACE'	=	0.0	Ft.
DIAJET'	=	2.30	Ft.
CIRCLE'	=	0.0	Ft.
$\alpha 1$	=	$0.0°$	
$\alpha 2$	=	$40.0°$	

RESULTS

Aircraft Runway Speed m.p.h.	Inlet-to-Freestream Velocity Ratio	Was Cross Ingestion Detected ?	Fluid Particle Time (Sec.)
90*	3.33	No	------
80	3.75	No	------
70	4.30	Yes	.15903
60	5.00	Yes	.21740
50	6.00	Yes	.39996
40	7.50	No	------

*Touchdown speed

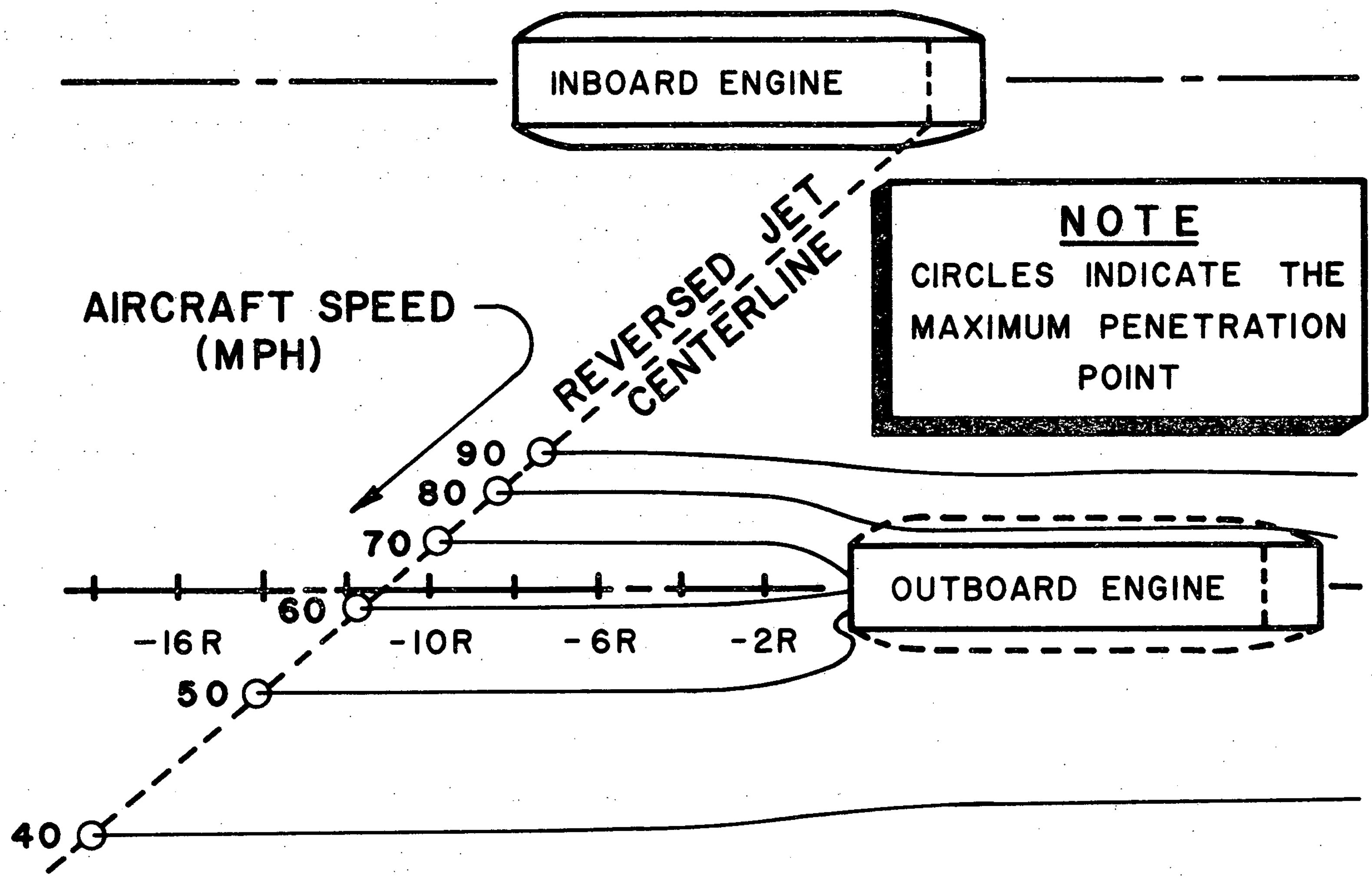

FIGURE 11. THE EXAMPLE PROBLEM

CHAPTER VII

CONCLUSIONS

This investigation succeeds in developing a method for analyzing the crosswind-free exhaust gas reingestion problem. The cases presented cover a wide range of nacelle aspect ratios and inlet-to-freestream velocity ratios and clearly demonstrate the generality of the computer program.

Results show the importance of using some type of singularity strength adjustment scheme in generating the inlet flow field model. At most points, the magnitude of the singularity-produced velocity required to establish the no-flow condition differs substantially from that of the normal velocity induced by the freestream-inlet combination.

Additionally, data suggests that the shape of the pre-entry streamtube is uninfluenced by the nacelle aspect ratio. It appears that the accuracy of the method is independent of the nacelle shape, as is assumed in the development of the inlet flow field model.

APPENDIX I

THE COMPUTER PROGRAM

```
C                                                                 ***********
C                                                                 * STEP 1  *
C                                                                 ***********
C
C     THE DIMENSIONING SECTION    ++++++++++++++++++++++++++++++++++++++++
C     DIMENSION VR(J1),VAX(J1),DPR(J1),DPX(J1),RADIAL(J1),AXIAL(J1)
          DIMENSION VR(21),VAX(21),DPR(21),DPX(21),RADIAL(21),AXIAL(21)
          DIMENSION KON4(21),KUN3(21)
          DIMENSION CHEKR(21),CHEKX(21)
C
C
C     THE INPUT SECTION         ++++++++++++++++++++++++++++++++++++++++++++
C     PROGRAM OPTIONS
C              (LAST,NOJET,NOCROS,NSPEED,NOCARD,NOPEST)
          LAST=2
          NOJET=0
          NOCROS=1
          NSPEED=0
          NOCARD=0
          NOPEST=0
C
C     PROGRAM INPUTS
C         (EP,DELTAX)
          EP=.01
C          INPUT DELTAX AS POSITIVE FOR FORWARD PLOTTING, NEGATIVE FOR
C        REVERSE.
          DELTAX=0,30000000000000000000
C
C     DYNAMIC INPUT
C              (UBA,VELRAT,VELJET)
          UBA=88.
          VELRAT=5.
          VELJET=880.000000000000000000000000
C
C     GEOMETRIC INPUT
C              (R,ALA,XJET,YJET,ZJET,ALPHA1,ALPHA2,XSPACE,YSPACE,ZSPACE,
C               DIAJET,CIRCLE)
          R=2.00000000000000
          ALA=22.6000000000000000000000
          XJET=20.0000000000000000000000
          YJET=2.000000000000000000000000
          ZJET=0.0000000
          ALPHA1=7.500000000000000
          ALPHA2=40.000000000000000000000000
          XSPACE=16.0000000000000000
          YSPACE=24.0000000000000000
          ZSPACE=0.00000000000000000000000
          DIAJET=2.300000000000000000000
          CIRCLE=0.00000000000000000
C
C     PROGRAM ADJUSTMENTS
C         (XCHEK,SLOPE,J6,J1,KLAST,DIV2,DIV4,N3STOP)
```

```
                XCHEK=50.
                SLOPE=.75
                J6=5
                J1=21
                KLAST=20
                DIV2=4.000000000000000000000
                DIV4=2.
                NSSTOP=6
C                                                               ***********
C                                                               * STEP 2  *
C                                                               ***********
C           INITIALIZATION I        ++++++++++++++++++++++++++++++++++++++++++++++
                DHOLD=DELTAX
                QS1=2.*VELRAT*U8A
                NSP=0
                VELGET=VELJET
                JLAST=J1-1
                DIV1=JLAST
                AL=ALA/R
                DX=AL/DIV1
                DSR=1./DIV1
                ILAST=JLAST
                DT1=6.28318/DIV1
                I1=ILAST+1
                K7=ILAST
                K8=I1
                NORAD=1
                NOAX=1
                OFF=0.
                KTEST=4*J1
  7011          CONTINUE
                OP5=1./(4.*3.14159*U8A)
                KON1=0
                KON5=1
                OUTPUT KON5
C
                IF(NOCARD.EQ.0)GO TO 2
                READ(5,396)VR
                READ(5,396)VAX
                DO 7008 J=1,J1
  7008          WRITE(6,383)VR(J),VAX(J)
                GO TO 7010
C                                                               ***********
C                                                               * STEP 3  *
C                                                               ***********
     2          KON1=KON1+1
                IF(KON1.GT.KLAST)GO TO 1007
                IF(LAST.EQ.1)WRITE(6,304)KON1
                IF(LAST.EQ.1)WRITE(6,300)
                IF(LAST.EQ.1)WRITE(6,305)
                IF(LAST.EQ.1)WRITE(6,300)
C
C           INITIALIZATION II       ++++++++++++++++++++++++++++++++++++++++++
                KONX=0
                KONR=0
                DO 3 J=1,J1
                AJ=J-1
                X=AJ*DX
                SR=AJ*DSR
                IF(J.GE.J1)X=X-DX*.5
                IF(J.GE.J1)SR=SR-DSR*.5
                IF(KON1.GT.1)GO TO 4
C
                CALL COOP(X,SR,KON5,A4,B4,A3,B3,SUM2,SUM3,SUM4,SUM5,DT1,OP14,T1,
              & RAD,NOAX,I1,AL,NZ,N4)
                AXIAL(J)=1.-QS1*OP5*AL*SUM3
```

```
          RADIAL(J)=-QS1*DP5*SUM2
          VAX(J)=-AXIAL(J)
          VR(J)=-RADIAL(J)
          IF(AXIAL(J))5,29,29
      5   WRITE(6,307)
          GO TO 1007
     29   IF(LAST.EQ.1)WRITE(6,306)J,OFF,RADIAL(J),OFF,OFF,OFF,AXIAL(J),O
        & OFF,OFF,OFF
          GO TO 3
C                                                              ***********
C                                                              * STEP 4  *
C                                                              ***********
      4   CALL STUFF(J,X,SR,VAX,VR,AL,DX,DSR,DT1,K7,K8,KON5,TRM33,TRM34,T
        & 5,TRM36,NORAD,NOAX,NZ,N4)
          TRM36=0.
          DPR(J)=TRM34+TRM35
          DPX(J)=TRM33+TRM36
          CHEKR(J)=DPR(J)+VR(J)+RADIAL(J)
          CHEKX(J)=DPX(J)+VAX(J)+AXIAL(J)
C                                                              ***********
C                                                              * STEP 5  *
C                                                              ***********
          IF(ABS(CHEKX(J)).LE.EP)GO TO 43
     53   KON4(J)=1
          GO TO 44
     43   KON4(J)=2
     44   IF(ABS(CHEKR(J)).LE.EP)GO TO 45
     51   KON3(J)=1;GO TO 46
     45   KON3(J)=2
     46   KONR=KONR+KON3(J)
          KONX=KONX+KON4(J)
          IF(LAST.EQ.2)GO TO 3
          WRITE(6,306)J,VR(J),RADIAL(J),TRM34,TRM35,VAX(J),AXIAL(J),TRM33,
        & M36,CHEKR(J),CHEKX(J)
      3   CONTINUE
          KSUM=KONX+KONR
          IF(LAST.EQ.2)GO TO 8000
          WRITE(6,300)
          WRITE(6,301)KSUM
          WRITE(6,303)KONR
          WRITE(6,302)KONX
          WRITE(6,300)
          WRITE(6,300)
   8000   CONTINUE
          IF(KSUM.GE.KTEST)GO TO 28
          IF(KON1.EQ.1)GO TO 2
C                                                              ***********
C                                                              * STEP 6  *
C                                                              ***********
          CALL STABLE(J1,KON4,KON3,CHEKX,CHEKR,VAX,VR)
          GO TO 2
C
     28   WRITE(6,313)KON1
          IF(LAST.GE.2)GO TO 7010
          GO TO 7007
C                                                              ***********
C                                                              * STEP 7  *
C                                                              ***********
   7010   CONTINUE
          IF(NOPEST.GT.0)GO TO 1602
          IF(NUJET.EQ.0.AND.NOCROS.EQ.0)GO TO 1008
   1602   CONTINUE
          VELJET=VELGET
          CALL THEJET(NOCROS,YJET,ZJET,ALPHA1,ALPHA2,DIAJET,VELJET,XJET,XM
        & ,RMPP,ZSPACE,YSPACE,XSPACE,XOP,RCROSS,U8A,R,THEATA,NSP,RJET)
C
```

```
 1008   KON5=2
        OUTPUT KON5
        N1=0
        KOOP1=1
        WRITE(6,314)
        NOPE=1
        NAL=0
        TIME1=0.
        IF(NOJET.EQ.1)GO TO 1437
        IF(NOCROS.GT.0)GO TO 1600
        IF(NOPEST.GT.0)GO TO 1437
 1603   CONTINUE
        READ(5,308)X,SR,TIME1
        GO TO 1438
 1437   X=XMPP
        SR=RMPP
        WRITE(6,397)X,SR
        SR=SR-CIRCLE/2.
        SLOPE2=(RJET-(DIAJET/2.)*COS(THEATA)-SR)/(XJET-X)
        BEE=SR-SLOPE2*X
        IF(NOPEST.GT.0)GO TO 1603
        GO TO 1601
 1600   X=XOP
        SR=RCROSS
 1601   CONTINUE
        NAL=ABS(X)/AL
        IF(NAL.GT.0)GO TO 1439
        NAL=1
 1439   RNAL=NAL
        DELTAX=(ABS(X))/(DIV1*RNAL)
C                                                                      ***********
C                                                                      * STEP 8  *
C                                                                      ***********
 1438   CONTINUE
        WRITE(6,308)X,SR,XCHEK
        KOOP2=XCHEK
        N2=1
        N3=0
        N4=1
        LESS=1
        XX1=0.0000000000
        XX2=DX
        NOGO=1
        DDX=0.00000000000000000000
        J5=0
        NTIM=0
        NZ=1
        NSSUM=0
        NZER=1
        EP2=ABS(DELTAX)
        EP3=-EP2/5.
        EP4=AL+EP2-EP3
        J3=10000
        IF(DELTAX)1022,1023,1023
 1022   J=J1+2
        J2=-2
        IF(X.LT.EP4)LESS=2
        GO TO 1006
 1023   J=-1;J2=2
        IF(X.GT.EP3)NOPE=2
 1006   IF(DELTAX)1040,1041,1041
 1040   IF(J3.EQ.J)GO TO 1020
        IF(X.LE.EP4.AND.LESS.EQ.1)GO TO 1042
        GO TO 1028
 1042   J3=J;GO TO 1028
 1041   IF(X.GE.EP3)GO TO 1020
```

```
      GO TO 1028
C
 1020 N2=2
      IF(J2)1025,1026,1026
 1025 X=AL-.5*DX;JSTOP=1;DELTAX=-2.*DX
      J3=1000
      GO TO 1024
C
 1026 IF(NOPE.EQ.2)GO TO 1502
      X=0.000000000000000000000000
 1502 JSTOP=J1
      J3=J1-2
      J=0;NDIV2=DIV2;NDIV3=DIV2/2.
      DELTAX=2.*DX/DIV2
      NOGO=2
      J28=1
      GO TO 1065
C
 1024 J=J+J2
      IF(J.EQ.JSTOP)GO TO 1045
      GO TO 1028
C
 1045 N2=3
      IF(J.EQ.1)GO TO 1027
      X=AL-.5*DX
      J3=1000
      RN3STP=N3STOP-2
      DELTAX=DHOLD/RN3STP
      N2=4
      GO TO 1028
C
 1027 DELTAX=DHOLD
      J=0
      X=0.
C
 1028 IF(SR.LE.0.)WRITE(6,386)
      IF(J.EQ.1.AND.SR.LE.1.00)GO TO 1203
      CALL COOP(X,SR,KUN5,A4,B4,A3,B3,SUM2,SUM3,SUM4,SUM5,DT1,DP14,T1,
     & RAD,NOAX,I1,AL,NZ,N4)
      IF(NORAD.EQ.2)GO TO 1048
      DPOTR=-QS1*DP5*SUM4
 1048 IF(NOAX.EQ.2)GO TO 1021
      DPOTX=1.-QS1*DP5*X*SUM5
C
 1021 CALL STUFF(J,X,SR,VAX,VR,AL,DX,DSR,DT1,K7,K8,KON5,TRM33,TRM34,TF
     & 5,TRM36,NORAD,NOAX,NZ,N4)
      IF(NORAD.EQ.2)GO TO 1049
      VRAD=DPOTR+TRM34+TRM35
      IF(NUGO.GT.2.AND.VRAD.GE.0.)VRAD=0.
 1049 IF(NUAX.EQ.2)GO TO 1050
      VAXY=DPOTX+TRM33+TRM36
 1050 GO TO(1051,1051,1066,1067,1076),N4
 1076 NORAD=1
 1051 IF(VAXY.LE.0.)WRITE(6,387)
      DRDX=VRAD/VAXY
      IF(ABS(VRAD).LE.EP)DRDX=0.
      IF(NOPE.EQ.1)GO TO 1500
C
      IF(VAXY.GE.0.)GO TO 1501
      NOPE=3
      GO TO 1101
 1501 NOPE=1
 1500 CONTINUE
C
C    SLOPE CHECK SECTION        ****************************************
      IF(NUGO.EQ.1)GO TO 1096
```

```
            IF(ABS(DRDX).LT.SLOPE)NSLOPE=1
            IF(ABS(DRDX).GE.SLOPE)NSLOPE=2
            IF(NSSUM.EQ.0)GO TO 1430
            IF(NZER.EQ.2.AND.N1.GT.0)GO TO 1096
            IF(N1.EQ.0)GO TO 1432
            NSSUM=NSSUM+NSLOPE
            GO TO 1096
 1430       NSHOLD=NSLOPE
            NSSUM=NSLOPE
            JHOLD=J
            XX1H=XX1
            XX2H=XX2
            VRHOLD=VRAD
            VXHOLD=VAXY
            DRDXH=DRDX
            NUMBER=1
            GO TO (1096,1402,1403,1404,1405,1406,1407),NOGO
 1402       IF(ABS(DRDX).GT.SLOPE)GO TO 1408
            IF(J.GE.J6)GO TO 1077
            GO TO 1096
 1403       IF(ABS(DRDX).LT.SLOPE)GO TO 1082
            GO TO 1096
 1404       IF(ABS(DRDX).GT.SLOPE)GO TO 1408
            GO TO 1096
 1405       IF(ABS(DRDX).LT.SLOPE)GO TO 1200
            GO TO 1096
 1406       IF(ABS(DRDX).GT.SLOPE)GO TO 1409
            GO TO 1096
 1407       IF(ABS(DRDX).GT.SLOPE)GO TO 1409
            GO TO 1096
 1432       IF(NSHOLD.EQ.2)GO TO 1429
            IF(NSSUM.LE.6)GO TO 1430
            X=XHOLD
            SR=SRHOLD
            NSHOLD=2
            GO TO 1431
 1429       IF(NSSUM.GE.6)GO TO 1430
            GO TO 1436
 1435       NUMBER=0
            NZER=1
 1436       X=SRHOLD
            SR=XHOLD
            NSHOLD=1
            VRAD=VRHOLD
            VAXY=VXHOLD
            DRDX=DRDXH
 1431       N1=0
            NSSUM=NSHOLD
            NUMBER=NUMBER+1
            IF(NUMBER.GE.3)GO TO 1433
            WRITE(6,399)
            WRITE(6,300)
            IF(J.EQ.JHOLD)GO TO 1434
            XX1=XX1H
            XX2=XX2H
            J=JHOLD
 1434       GO TO(1096,1408,1082,1408,1200,1409,1409),NOGO
 1433       WRITE(6,398)
            GO TO 1007
C
 1096       CONTINUE
            CALL RUNGE(X,SR,XHOLD,SRHOLD,DRDX,DELTAX,J3,AL,EK1,EK2,EK3,EK4,N
     &      J,DX,DDX,J5,NOGO,XX1,VAXY,VRAD,EP,NZER)
            IF(NZER.EQ.2)GO TO 1435
            GO TO(1012,1075,1075,1013),N1
 1075       GO TO(1028,1073,1086,1080,1103,1080,1073),NOGO
```

```
      GO TO 1028
 1012 CONTINUE
      GO TO(1028,1073,1086,1080,1103,1080,1073),NOGO
      GO TO 1028
 1013 WRITE(6,383)X,SR
      WRITE(6,300)
      N1=0
C
      IF(NOJET.GT.0.OR.NOCROS.GT.0)GO TO 1413
      IF(NOPEST.EQ.0)GO TO 1097
      IF(NAL.EQ.-10)GO TO 7009
      BORDER=SLOPE2*X+BEE
      IF(SR.GT.BORDER)NAL=-10
      IF(NAL.EQ.-10)WRITE(6,395)
 1413 CALL TIME(NTIM,XA,XB,RA,RB,VPA,VPB,X,SR,VAXY,VRAD,TIME1,TIME2)
 7009 CONTINUE
C
 1097 GO TO(1083,1062,1086,1062,1103,1062,1062),NOGO
C
 1083 KOOP1=KOOP1+1
      IF(KOOP1-KOOP2)1029,1029,7007
 1029 GO TO(1006,1024,1028,1046),N2
 1046 N3=N3+1
      IF(N3.LT.N3STOP)GO TO 1028
      DELTAX=DHOLD
      N2=3
      GO TO 1028
C
 1065 J4=0
 1061 J5=0
      J=J+J2B
      IF(J2B.LT.1)GO TO 1100
      IF(J.EQ.1)GO TO 1094
      XX1=XX2
      IF(J.EQ.1)XX1=0.0000000000
      XX2=XX1+DX
 1094 IF(NOGO.EQ.3)GO TO 1084
      GO TO 1074
 1100 XX2=XX1
      XX1=XX2-DX
      IF(J.EQ.2)XX1=0.000000000000000000
      IF(J.LT.1.AND.N1.EQ.0)GO TO 1203
      IF(NOGO.EQ.5)GO TO 1084
 1074 N4=2
      IF(NOPE.EQ.1)GO TO 1028
      NTRY=2
      GO TO 1087
 1062 J4=J4+1
      IF(J4.EQ.NDIV3.AND.NOGO.EQ.4)GO TO 1081
      IF(J4.EQ.NDIV2.AND.NOGO.EQ.4)GO TO 1081
 1202 IF(J4.EQ.NDIV2.AND.NOGO.EQ.6)GO TO 1201
      IF(J4.EQ.NDIV3.AND.NOGO.EQ.6)GO TO 1201
 1092 IF(J4.EQ.NDIV3)GO TO 1061
      IF(J4.EQ.NDIV2)GO TO 1065
 1073 IF(J5.EQ.NDIV2)GO TO 1074
      GO TO 1080
C
 1077 NOGO=1
      N4=1
      DELTAX=2.*DX
      GO TO 1096
C
 1081 NOGO=2
      DELTAX=2.*DX/DIV2
      J2B=1
      GO TO 1092
```

```
C
 1408     NTRY=1
 1087     NOGO=3
          XMAX=.999*X
          J28=1
          IF(J4.LE.NDIV3)GO TO 1093
 1105     J4=NDIV3
          DP1200=-1.
          GO TO 1106
 1093     J4=0
          DP1200=1.
C      NEXT CARD GETS A DELTA R FOR THE FLIPPED RUNGE-KUTTA METHOD
 1106     DELTAX=-DX/(DIV4*DIV2)
          IF(NTRY.EQ.1)GO TO 1410
          IF(NOPE.EQ.3)GO TO 1501
          IF(NOGO.EQ.5)GO TO 1103
          GO TO 1086
 1084     J4=J4+DP1200*NDIV3
          DP1200=-DP1200
          IF(NOGO.EQ.5)GO TO 1103
 1086     IF(X.GE.XX2)GO TO 1061
          IF(X.LT.XMAX.AND.N1.EQ.0)GO TO 1428
 1425     XMAX=X
          GO TO 1107
 1427     IF(VAXY)1426,1426,1087
 1428     IF(VAXY)1101,1425,1425
 1103     IF(X.LE.XX1)GO TO 1061
          IF(X.GT.XMIN.AND.N1.EQ.0)GO TO 1427
 1426     XMIN=X
 1107     IF(SR.GE.1.01)GO TO 1080
          WRITE(6,388)
          GO TO 7007
C
 1082     NOGO=4
          DELTAX=2.*(XX2-X)/DIV2
          J28=1
          J5=0
          GO TO 1096
C
 1409     NTRY=1
 1101     NOGO=5
          XMIN=1.001*X
          J28=-1
          IF(J4.GE.NDIV3)GO TO 1093
          GO TO 1105
C
 1200     NOGO=6
          DELTAX=-2.*(X-XX1)/DIV2
          J5=0
          J28=-1
          GO TO 1096
C
 1201     NOGO=7
          DELTAX=-2.*DX/DIV2
          J28=-1
          GO TO 1092
C
 1080     N4=3
          NOAX=2
          XX3=X
          X=XX1
          GO TO 1028
 1066     N4=4
          X=XX2
          VR1=VRAD
          GO TO 1028
```

```
 1067   N4=5
        X=XX3
        VR2=VRAD
        VRAD=((DX-DDX)/DX)*(VR1-VR2)+VR2
        NOAX=1
        NORAD=2
        GO TO 1028
C
 1410   NTRY=2
        GO TO 1096
C                                                         ***********
C                                                         * STEP 9  *
C                                                         ***********
 1203   WRITE(6,390)
        TIME1=TIME1*R/U8A
        IF(NOJET.GT.0)WRITE(6,391)TIME1
        IF(NUCROS.GT.0)WRITE(6,392)TIME1
        IF(NOJET.EQ.0.AND.NOCROS.EQ.0)WRITE(6,394)
        GO TU 7007
C                                                         ***********
C                                                         * STEP 10 *
C                                                         ***********
 7007   IF(NSPEED.EQ.0)GO TO 1007
        NSP=NSP+1
        IF(NSP.EQ.NSPEED)GO TO 1007
        READ(5,396)U8A
        GO TO 7011
 1007   STOP
  300   FORMAT('0')
  301   FORMAT('KSUM=',I5)
  302   FORMAT('KONX=',I5)
  303   FORMAT('KONR=',I5)
  304   FORMAT('KON1=',I5)
  305   FORMAT('          J          VR          RADIAL          VR-RAD          V
      & AX        VAX          AXIAL        VAX-RAD          VAX-AX    CHEKR    CHE
      & ')
  306   FORMAT(2X,I10,8(2X,F10.5),2(2X,F6.3))
  307   FORMAT('THE NACELLE CAN NOT BE GENERATED')
  308   FORMAT(3F10.5)
  313   FORMAT('THE INLET FLOW FIELD MODEL HAS BEEN GENERATED.  THE NUMB
      &  OF ITERATIONS REQUIRED WAS',I5)
  314   FORMAT('      X          SR      XCHEK')
  383   FORMAT(8F10.5)
  386   FORMAT('THE RADIUS HAS BECOME NEGATIVE')
  387   FORMAT('THE AXIAL VELOCITY HERE IS NEGATIVE')
  388   FORMAT('THE RADIUS HAS PENETRATED THE NACELLE')
  390   FORMAT('THE STREAMLINE HAS ENTERED THE INLET')
  391   FORMAT('EXHAUST GAS RE-INJESTED',F8.5,     'SECONDS AFTER PENETR
      & ION OF THE PRE-ENTRY STREAM TUBE')
  392   FORMAT('EXHAUST GAS CROSS-INJESTED',F8.5,     'SECONDS AFTER PEN
      & RATION OF THE PRE-ENTRY STREAM TUBE')
  394   FORMAT('EXHAUST GAS  INJESTION WAS NOT DETECTED')
  395   FORMAT('SECTIONS OF THE ENTRAINMENT PORTION OF THE JET LIE WITHI
      & THE PRE-ENTRY STREAM TUBE')
  396   FORMAT(8F10.5)
  397   FORMAT('THE MAXIMUM PENETRATION POINT OCCURS AT',F10.5,        '
      & DII AXIALLY AND',F10.5,        'RADII RADIALLY')
  398   FORMAT('THE POINT IS CURRENTLY UNOBTAINABLE')
  399   FORMAT('PROCEDURE CHANGED AT THIS POINT.  ABOVE NUMBERS ARE NO G
      & D')
        END
```

```
      SUBROUTINE TIME(NTIM,XA,XB,RA,RB,VPA,VPB,X,SR,VAXY,VRAD,TIME1,TI
     & 2)
C     THIS SUBROUTINE CALCULARES DIMENSIONLESS TIME
      IF(NTIM.EQ.0)GO TO 1
      XA=XB
      RA=RB
      VPA=VPB
    1 XB=X
      RB=SR
      VPB=SQRT(VAXY**2+VRAD**2)
      IF(NTIM.EQ.0)GO TO 2
      GO TO 3
    2 NTIM=1
      GO TO 5000
    3 VAB=(VPA+VPB)/2.
      XAB=XA-XB
      RAB=RA-RB
      DSAB=SQRT(XAB**2+RAB**2)
      TAB=DSAB/VAB
      TIME1=TIME1+TAB
 5000 RETURN
      END
```

```
      SUBROUTINE RUNGE(X,SR,XHOLD,SRHOLD,DRDX,DELTAX,J3,AL,EK1,EK2,EK
     & K4,N1,J,DX,DDX,J5,NOGO,XX1,VAXY,VRAD,EP,NZER)
C     THIS SECTION CONTAINS THE RUNGE-KUTTA METHOD.
      N1=N1+1
      IF(NOGO.EQ.3.OR.NOGO.EQ.5)GO TO 6
      GO TO 1079
    6 N5=1
      IF(ABS(VRAD).LE.EP)GO TO 7
      DRDX=VAXY/VRAD
      IF(ABS(VAXY).LE.EP)DRDX=0.
      GO TO 2
    7 NZER=2
      GO TO 5000
    5 N5=3
      GO TO 2
    4 J5=J5+2
    3 DDX=X-XX1
      GO TO 5000
 1078 N5=2
    2 XSWAP=X
      RSWAP=SR
      X=RSWAP
      SR=XSWAP
      GO TO(1079,5000,3),N5
 1079 GO TO(1016,1017,1018,1019),N1
 1016 EK1=DRDX*DELTAX
      IF(J3.EQ.1000)GO TO 1043
 1044 XHOLD=X
      SRHOLD=SR
      X=X+DELTAX/2.
      SR=SR+EK1/2.
      GO TO(5000,3,5,3,5,3,3),NOGO
 1043 X=AL;J3=10000;GO TO 1044
 1017 EK2=DRDX*DELTAX
      SR=SRHOLD+EK2/2.
      GO TO(5000,5000,1078,5000,1078,5000,5000),NOGO
 1018 EK3=DRDX*DELTAX
      X=XHOLD+DELTAX
      IF(J.EQ.J3)X=AL-.5*DX
```

```
            SR=SRHOLD+EK3
            GO TO(5000,4,5,4,5,4,4),NOGO
 1019       EK4=DRDX*DELTAX
            DELRAD=(EK1+2.*EK2+2.*EK3+EK4)/6.
            X=XHOLD+DELTAX
            SR=SRHOLD+DELRAD
            GO TO(5000,5000,1078,5000,1078,5000,5000),NOGO
 5000       RETURN
            END
```

```
            SUBROUTINE THEJET(NOCROS,YJET,ZJET,ALPHA1,ALPHA2,DIAJET,VELJET,X
     &      T,XMPP,RMPP,ZSPACE,YSPACE,XSPACE,XOP,RCROSS,U8A,R,THEATA,NSP,RJE
C      THIS SECTION CONTAINS THE LOCKHEED CORRELATION.
            IF(NSP.GT.0)GO TO 200
            XJET=XJET/R
            YJET=YJET/R
            ZJET=ZJET/R
            DIAJET=DIAJET/R
            ALPHA1=ALPHA1/57.29578
            ALPHA2=ALPHA2/57.29578
  200       CONTINUE
            VELJET=VELJET/U8A
            RJET=SQRT(YJET**2+ZJET**2)
            IF(ALPHA2.LT..01)GO TO 1
            BETA=ATAN(TAN(ALPHA1)/SIN(ALPHA2))
            IF(ALPHA1.LT..01)BETA=0.000000000000000
            GO TO 2
    1       BETA=90.000/57.29578
    2       CONTINUE
            THEATA=ACOS(COS(ALPHA1)*COS(ALPHA2))
            A=(1.-.734*(SIN(THEATA))**.685)
            PMPP=2.97*DIAJET*A*(VELJET**.94)
            QMPP=PMPP*TAN(THEATA)
            XMPP=XJET-PMPP
            RMPP=SQRT(RJET**2+QMPP**2+2.*QMPP*(YJET*COS(BETA)+ZJET*SIN(BETA)
            OUTPUT XMPP,RMPP
            IF(NOCROS.EQ.0)GO TO 5000
            IF(NSP.GT.0)GO TO 205
            XSPACE=XSPACE/R
            YSPACE=YSPACE/R
            ZSPACE=ZSPACE/R
  205       CONTINUE
            ZMPP=RMPP*SIN(BETA)
            ZOP=ZSPACE+ZMPP
            YMPP=RMPP*COS(BETA)
            YOP=YSPACE-YMPP
            XOP=XMPP-XSPACE
            RCROSS=SQRT(YOP**2+ZOP**2)
 5000       RETURN
            END
```

```
            SUBROUTINE STABLE(J1,KON4,KON3,CHEKX,CHEKR,VAX,VR)
            DIMENSION KON4(J1),KON3(J1),CHEKX(J1),CHEKR(J1),VAX(J1),VR(J1)
C      THIS SECTION ADJUSTS THE COMPENSATORY SINGULARITY STRENGTHS.
   40       DO 42 I=1,J1
            IF(KON4(I).GE.2)GO TO 47
            A102=CHEKX(I)/2.
            IF(VAX(I)*CHEKX(I))64,64,62
```

```
 62      IF(ABS(VAX(I))-ABS(A102))63,63,64
 63      VAX(I)=VAX(I)/2.05
         GO TO 47
 64      VAX(I)=VAX(I)-A102
 47      IF(KUN3(I).GE.2)GO TO 42
         A101=CHEKR(I)/2.
         IF(VR(I)*CHEKR(I))61,61,56
 56      IF(ABS(VR(I))-ABS(A101))60,60,61
 60      VR(I)=VR(I)/2.05
         GO TO 42
 61      VR(I)=VR(I)-A101
 42      CONTINUE
         RETURN
         END
```

```
         SUBROUTINE STUFF(J,X,SR,VAX,VR,AL,DX,DSR,DT1,K7,K8,KON5,TRM33,TF
       & 4,TRM35,TRM36,NORAD,NOAX,NZ,N4)
C      THIS SECTION COMPUTES THE COMPENSATORY TERMS USED IN EQS. 5 & 6.
         DIMENSION VR(21),VAX(21)
 309     FORMAT('DIV BY ZERO.......OP74 AND OP81 IN STUFF')
 310     FORMAT('DIV BY ZERO......OP76 AND OP83 IN STUFF')
 311     FORMAT('NEG SQRT.....OP74 AND OP81 IN STUFF')
 312     FORMAT('NEG SQRT..... OP76 AND OP83 IN STUFF')
         TRM33=0.;TRM34=0.;TRM35=0.;TRM36=0.
         OP30=(1./(2.*3.14159))*DT1
         OP30A=OP30*DX
         OP30B=OP30*DSR
C
         DO 22 K11=1,K8
C
         IF(K11.EQ.1.OR.K11.EQ.K8)OP71=0.5
         AK11=K11-1
         X1=DX*AK11
         SR3=DSR*AK11
         IF(K11.GE.K8)X1=X1-DX*.5
         IF(K11.GE.K8)SR3=SR3-DSR*.5
         OP77=0.;OP78=0.;OP84=0.;OP85=0.
         DO 21 K9=1,K7
         AK9=K9-1
         T1=DT1*AK9
         IF(KON5.EQ.1)RS=1.
         IF(KON5.EQ.2)RS=SR
         OP100=((X-AL)**2+RS**2-2.*RS*SR3*COS(T1)+SR3**2)**3
         IF(KON5.GT.1)GO TO 33
         IF(OP100)953,953,34
 33      IF(OP100)917,909,34
 34      OP73=SQRT(OP100)
         IF(NURAD.EQ.2)GO TO 1
         OP74=VAX(K11)*(RS-SR3*COS(T1))*SR3/OP73
         GO TO 910
 953     OP74=0.;GO TO 910
 917     OP74=0.;WRITE(6,311);GO TO 910
 909     OP74=0.;WRITE(6,309)
 910     OP77=OP77+OP74
C
C      UNIT 1........OP=CAX/DX...........TRM36...............++++++++++++
         IF(KON5.EQ.1)GO TO 938
 1       IF(NUAX.EQ.2)GO TO 32
         IF(OP100.LE.0.)GO TO 911
         OP81=VAX(K11)*(X-AL)*SR3/OP73
         GO TO 912
 911     OP81=0.
```

```
  912   OP85=OP85+OP81
   23   IF(KON5.GT.1)GO TO 32
C
C     UNIT 3........DP=CR/DX............TRM33...............++++++++++++
  938   IF(X1.GE.AL)GO TO 952
        OP82=((AL-X1)**2+SR**2-2.*SR*COS(T1)+1.)**3
        IF(OP82)952,952,36
   32   OP82=((X-X1)**2+SR**2-2.*SR*COS(T1)+1.)**3
        IF(NOAX.EQ.2)GO TO 2
        IF(OP82)918,913,36
   36   OP75=SQRT(OP82)
        IF(KON5.LE.1)GO TO 937
        OP76=VR(K11)*(X-X1)/OP75
        GO TO 914
  937   OP76=VR(K11)*(AL-X1)/OP75
        GO TO 914
  952   OP76=0.;GO TO 914
  918   OP76=0.;WRITE(6,312);GO TO 914
  913   OP76=0.;WRITE(6,310)
  914   OP78=OP78+OP76
        IF(NORAD.EQ.2)GO TO 21
C
        IF(KON5.LT.2)GO TO 919
        IF(OP82.LE.0.)GO TO 915
        GO TO 5
    2   IF(OP82)915,915,6
    6   OP75=SQRT(OP82)
    5   CONTINUE
C     UNIT 4........DP=CR/DR............TRM34..............++++++++++++
        OP83=VR(K11)*(SR-COS(T1))/OP75
        GO TO 916
  919   OP82=((X-X1)**2-2.*COS(T1)+2.)**3
        IF(OP82)915,915,80
   80   OP75=SQRT(OP82)
        OP83=VR(K11)*(1.-COS(T1))/OP75
        GO TO 916
  915   OP83=0.
  916   OP84=OP84+OP83
C
   21   CONTINUE
C
        IF(NORAD.EQ.2)GO TO 3
        TRM34=TRM34+OP71*OP84
        TRM35=TRM35+OP71*OP77
    3   IF(NOAX.EQ.2)GO TO 22
        TRM33=TRM33+OP71*OP78
        IF(KON5.LT.2)GO TO 22
        TRM36=TRM36+OP71*OP85
C
   22   OP71=1.
C
        IF(NORAD.EQ.2)GO TO 4
        TRM34=TRM34*OP30A
        TRM35=TRM35*OP30B
    4   IF(NOAX.EQ.2)GO TO 951
        TRM33=TRM33*OP30A
        IF(KON5.LT.2)GO TO 951
        TRM36=TRM36*OP30B
C
  951   RETURN
        END
```

```
      SUBROUTINE COOP(X,SR,KON5,A4,B4,A3,B3,SUM2,SUM3,SUM4,SUM5,DT1,OP
     & ,T1,NORAD,NOAX,I1,AL,NZ,N4)
C     THIS SECTION COMPUTES THE FREESTREAM-INLET INDUCED VELOCITY TERMS.
  307 FORMAT('DIV BY ZERO....OP13 EQ....IN COOP')
      SUM2=0.;SUM3=0.;SUM4=0.;SUM5=0.
      DO 6 I=1,I1
      AI=I-1
      IF(I.EQ.1.OR.I.EQ.I1)OP14=0.5
      T1=DT1*AI
      IF(KON5.EQ.2)GO TO 2
      A4=AL**2+SR**2
      B4=-2.*SR*COS(T1)
      A3=X**2+1.
      B3=-2.*COS(T1)
      GO TO 3
    2 A4=X**2+SR**2
      B4=-2.*SR*COS(T1)
      A3=A4
      B3=B4
    3 CONTINUE
      A1=A3;B1=B3;A2=A4;B2=B4
      IF(NOAX.EQ.2)GO TO 1
  929 A5=4.*A2-B2**2
      IF(A5.EQ.0.)GO TO 933
      OP13=(1./(4.*A2-B2**2))*(4.*SQRT(A2)-((2.*B2+4.*A2)/SQRT(A2+B2+1
     & ))
      OP16=OP14*OP13*DT1
      GO TO 935
  933 OP16=0.;WRITE(6,307)
  935 IF(KON5.GE.2)GO TO 930
      SUM3=SUM3+OP16
      SRR=1.
      GO TO 931
  930 SUM5=SUM5+OP16
    1 IF(NORAD.EQ.2)GO TO 939
      SRR=SR
  931 OP1=4.*A1-B1**2
      IF(ABS(OP1).LE..001)OP1=.0000000000000000000000000000
      IF(OP1.EQ.0.)GO TO 900
      OP9=(1./(4.*A1-B1**2))
      OP10=((2.*B1**2-4.*A1+2.*A1*B1)/(SQRT(A1+B1+1.)))-2.*B1*SQRT(A1)
      OP7=OP9*(4.*SQRT(A1)-((2.*B1+4.*A1)/(SQRT(A1+B1+1.))))*SRR
      OP201=SQRT(A1)+B1/2.
      IF(OP201)900,900,2001
 2001 OP11=ALOG((SQRT(A1+B1+1.)+B1/2.+1.)/OP201)
      OP8=COS(T1)*(OP9*OP10+OP11)
      OP12=OP7-OP8
      OP15=OP14*OP12*DT1
      GO TO 903
  900 OP15=0.
  903 IF(KON5.GE.2)GO TO 932
      SUM2=SUM2+OP15
      GO TO 939
  932 SUM4=SUM4+OP15
  939 CONTINUE
    6 OP14=1.
 3003 RETURN
      END
```

APPENDIX II

PROCEDURE FOR INPUTTING COMPUTER PROGRAM VARIABLES

The Program Options

LAST - This quantity is inputted as 2 for normal operations and inputted as 1 if only the nacelle generation sections of the program are to be operated.

NOJET - Inputted as 1 if reingestion is to be studied; otherwise 0.

NOCROS - Inputted as 1 if cross-ingestion is to be studied, otherwise 0.

NSPEED - Inputted as 0 if only one aircraft speed is to be studied. Otherwise the value of this quantity is the number of aircraft speeds to be studied.

NOCARD - Inputted as 0 if nacelle generation sections are to be used. If this quantity is set equal to 1, the singularity-produced velocities are read in on computer cards, rather than determined in the program.

NOPEST - Inputted as 1 if the program is to determine whether or not the entraining portion of the reversed jet lies within the pre-entry streamtube. Otherwise, inputted as 0.

Of the terms NOJET, NOCROS, and NOPEST, only one can be non-zero during a particular study.

The Program Inputs

EP - The degree of accuracy to which the no-flow condition is satisfied.

DELTAX - The dimensionless incremental value of x used in the streamline computational section. If this quantity is inputted as positive the streamlines will be calculated in the direction of the freestream flow. If "DELTAX" is negative, the opposite direction is used.

The Dynamic Input

U8A - The dimensional velocity of the aircraft. If more than one velocity is to be studied, the highest velocity is inputted here.

VELRAT - The inlet-to-freestream velocity ratio. If more than one velocity is to be studied, the lowest velocity ratio is inputted here.

VELJET - The dimensional reversed jet velocity.

The Geometric Input

ALA - The dimensional nacelle length.

Circle - This quantity expands the concept of the Maximum Penetration Point from a point to an area. "CIRCLE" is inputted as the dimensionless diameter of a circle with the center at the Maximum Penetration Point. If this concept is not to be used, the quantity is inputted as zero.

The remaining terms in this section have the same meaning as in the main body of this report, but must be inputted in dimensional form.

BIBLIOGRAPHY

1. Tatom, J. W., et al. "A Study of Jet Impingement on Curved Surfaces Followed by Oblique Introduction Into a Free-stream Flow," 1st Annual Progress Report under NASA Grant NGR 43-002-034, Vanderbilt University, December, 1971.

2. Keffler, J. F., and Baines, W. D. "The Round Turbulent Jet in a Cross-Wind," Journal of Fluid Mechanics, Vol. 15, Part 4, pp. 481-496, 1968.

3. Weiss, D. C. and McGuigan, W. M. "In-Flight Thrust Control for Fighter Aircraft," AIAA Paper 70-513, 1970.

4. Cooper, M. A. Temperature Field of the Two-Dimensional Transverse Hot Air Jet In a Freestream Flow, Masters Thesis, Vanderbilt University, January, 1972.

5. Hayden, T. K. Velocity Field of the Two-Dimensional Transverse Hot Air Jet in a Freestream Flow, Masters Thesis, Vanderbilt University, May, 1972.

6. Smith, A.M.O., and Pierce, J. "Exact Solution of the Neuman Problem Calculation of Non-Circulatory Plane and Axial Symmetric Flows About or Within Arbitrary Bodies," Douglas Aircraft Report No. ES 26988, 1958.

7. Hopkins, D. F., and Robertson, J. M. "Two-Dimensional Incompressible Fluid Jet Penetration," J. Fluid Mech., Vol. 29, Part 2, pp. 273-287, 1967.

8. Strand, T., and Wei, M.H.Y. "Linearized Inviscid Flow Theory of Two-Dimensional Thin Jet Penetration Into a Stream," AIAA J. of Aircraft, 1968.

9. Ehrich, F. F., "Penetration and Deflection of Jets Oblique to a General Stream," J. of Aero. Sciences, February, 1953.

10. Tatom, J. W., and Searle, N. Development Authorization 4-7131-1006, "Thrust Reverser Positive Pitch," Lockheed-Georgia Company, April 3, 1968.

11. Margason, R. J. "The Path of a Jet Directed at Large Angles to a Subsonic Freestream," NASA TND-4919, November, 1968.

12. Tatom, F. B., et al. "Study Effect of Engine Ignition on Airflow Over Vehicle," Northrop Space Laboratories, Research and Analysis Section Tech. Memo #43, December, 1964.

13. Robertson, J. M. Hydrodynamics in Theory and Application, Prentice-Hall, Englewood Cliffs, 1965.

14. Wylie, Jr., C. R. Advanced Engineering Mathematics, McGraw-Hill, New York, 1951.

15. Valentine, H. R. Applied Hydrodynamics, 2nd Edition, Plenum Press, New York, 1967.

16. Scarbourough, J. B. Numerical Mathematical Analysis, 6th Edition, John Hopkins Press, Baltimore, 1966.